Available online at www.sciencedirect.com

ScienceDirect

Underground Space 13 (2023) 205–227

www.keaipublishing.com/undsp

Review of analytical methods for stress and deformation analysis of buried water pipes considering pipe-soil interaction

Yingxu Huo [a], Sherif Mohsen Mohamed Hassan Gomaa [b,c,*], Tarek Zayed [b], Mohamed Meguid [d]

[a] Department of Civil and Environmental Engineering, The Hong Kong Polytechnic University, Hung Hom, Hong Kong 999077, China
[b] Department of Building and Real Estate, The Hong Kong Polytechnic University, Hung Hom, Hong Kong 999077, China
[c] Structural Engineering Department, Faculty of Engineering, Mansoura University, Mansoura 35516, Egypt
[d] Department of Civil Engineering, McGill University, Montreal, Quebec H3A 0G4, Canada

Received 28 September 2022; received in revised form 18 January 2023; accepted 18 February 2023
Available online 5 July 2023

Abstract

Buried water pipelines are vulnerable to fail or break due to excessive loading or ground displacements. Accurate evaluation of pipe performance and serviceability relies on the proper understanding of pipe-soil interactions (PSI). Analytical methods are important approaches to studying PSI. However, a systematic and thorough literature review to analyze the existing research trends, technological achievements and future research opportunities is not available. This work investigates analytical methods that analyze the stress and deformation of pipes in terms of cross-sectional, transverse and longitudinal PSI problems. First, scientometric analysis is performed to acquire relevant research works from online databases and analyze the existing data of influential authors, productive research sources and frequent key word occurrence in the fields of interest. Second, a qualitative discussion is performed in the three categories of PSI: (1) cross-sectional, including ovalization and circumferential behaviours; (2) transverse, including seismic fault crossing, weak soil zones, ground settlement and pipe uplift; and (3) longitudinal. Third, six research opportunities are discussed, including the role of friction in cross-sectional deformation, combined effects of bending and compression, choice of soil reaction models and calibration of key parameters, effect of pipe flaws, soil spatial variability and behaviours of curved pipes. This study helps beginners familiarize themselves with PSI analytical methods and provides experienced researchers with ideas for future research directions.

Keywords: Pipeline; Analytical methods; Pipe-soil interactions; Seismic fault; Settlement; Uplift; Buckling; Tunnelling

1 Introduction

Underground water pipelines are indispensable infrastructures that guarantee normal, fast and secure delivery of essential public need. Globally, pipeline operation always faces many challenges and leads to pipe failure in many cases. For example, the Water Supplies Department (WSD) of Hong Kong reported 88 cases of water pipe bursts and 8512 cases of pipe leakage in 2017, and a leakage rate of 15% in 2021 (WSD, 2022). There have been extensive reports of pipe failure due to ground displacements, such as induced by tunnelling (Hou et al., 2015), excavation (Yoo et al., 2005), landslides (Akagawa et al., 2012), frost heave (Palmer & Williams, 2003; Xu et al., 2010) and earthquakes (O'Rourke & Liu, 1999; Cubrinovski et al., 2011; Tokimatsu et al., 2012). Some types of pipe failure modes, such as circumferential break, joint leakage, longitudinal cracking have been identified as a result of the aforementioned ground displacements. For example, circumferential cracks could result from axial tensile stress due to pipe bending or axial elongation; longitudinal split/cracking mostly occurs from circumferential or hoop stress; bell split or joint failure normally takes place

* Corresponding author.
E-mail address: sherif.gomaa@polyu.edu.hk (S.M.M.H. Gomaa).

https://doi.org/10.1016/j.undsp.2023.02.017
2467-9674/© 2023 Tongji University. Publishing services by Elsevier B.V. on behalf of KeAi Communications Co. Ltd.
This is an open access article under the CC BY-NC-ND license (http://creativecommons.org/licenses/by-nc-nd/4.0/).

due to differential thermal loads between pipe and joint materials (Rajani et al., 1996; Makar et al., 2020; Rajeev et al., 2014; Barton et al., 2019). Hence, evaluating the stress and deformation of buried water pipes considering the pipe-soil interaction (PSI) is a vital task in pipeline engineering. Proper understanding of PSI is still a major issue because pipes obtain supports as well as carry loads from surrounding soils. Evaluating the performance and failure susceptibility of pipelines under different ground conditions has been an important topic among geotechnical engineers and academia.

Stress and deformation of pipes induced by external loads have been studied through experimental, numerical and analytical methods. Experimental studies on PSI usually involve a model pipe whose size is much smaller than the pipe in situ. (Hsu et al., 2001, 2006), since field conditions are difficult to be reproduced in laboratories. To overcome this, centrifuge modelling may be applied to simulating the in situ stress conditions and pipe performance subject to, for example, fault-crossing (Saiyar et al., 2016). Full-scale experiment is also a choice to investigate the pipe performance (Sheil et al., 2021; Qin et al., 2021). Fibre optic sensing, strain gauges and load cells are popular tools to measure the stresses and strains of pipes (Ni et al., 2018a; Qin et al., 2021; Saiyar et al., 2016). Numerical methods studying PSI are dependent on the purposes of study. Most studies have involved the continuum-based finite element method (FEM) that simulates the pipe as a beam, which can study the flexural and longitudinal deformation of the pipe (Cocchetti et al., 2009; Ni et al., 2018b; Qin & Ni, 2019; Qin et al., 2019, 2021, 2022; Zhai et al., 2022). Shell model can further be used to investigate the cross-sectional deformation of a pipe, while it requires much more computational resources than the beam model. Therefore, pipe segments with large cross-sectional deformation (e.g., segments that are close to fault crossing) are usually modelled as shell elements and other segments can be simplified as beams (Takada et al., 2001; Liu et al., 2004; Saberi et al., 2013). Fragility analysis, which investigates the risks of pipe failure subject to geo–hazards, can be performed through FEM modelling as well with the help of machine learning techniques (Ni & Mangalathu, 2018a; Ni et al., 2018, 2020;). The soil reactions in these FEM models are usually modelled through the Mohr–Coulomb criterion. Alternatively, if the purpose of study is to examine the pipe-soil interaction at a microscopic scale, discrete element method (DEM) is an appropriate tool which gives insights to soil particle displacements and force chains (Calvetti et al., 2004; Marshall et al., 2010; Macaro et al., 2021). Compared to the former two methods, the analytical approach holds the merits that it does not require complex experimental conditions and apparatus. Besides, it requires very few computational resources and the results can be computed fast with an acceptable accuracy. Moreover, it helps understand the physical rationale and the basic fundamentals of how pipe interacts with soil. The analytical methods also have a close connection with design procedures and codes. For example, ALA (2001) adopted the analytical method proposed by Hetényi and Hetbenyi (1946) to analyze the flexural performance of a pipe, which assumes the pipe is a long beam rested on elastic foundations. Conversely, Paolucci et al. (2010) referred the values of soil resisting force to those suggested in ALA (2001) when analyzing the pipe performance subject to seismic fault. Therefore, many researchers have attempted to study PSI under different ground conditions through analytical approach. According to the problem of interest, this work classifies the analytical approach into cross-sectional, transverse (including vertical) and longitudinal pipe performance. In cross-sectional analysis, the problems of interest are usually the pipe ovalization (Masada, 2000; Masada & Sargand, 2007) induced by soil backfill loads or circumferential stress and strains (Rajani et al., 1996; Rajani & Tesfamariam, 2004). Estimation of ovalization has been predominantly based on the famous Iowa approach (Watkins & Spangler, 1958). In transverse analysis, the main focus is usually on the pipe bending performance induced by surface loads (Wang & Moore, 2014; Wang & Moore, 2015), landslides (Chaudhuri & Choudhury, 2020; Cocchetti et al., 2009), seismic faults (Karamitros et al., 2007; Trifonov & Cherniy, 2010), partial loss of soil support (Rajani & Tesfamariam, 2004), tunnelling and mining-induced ground settlement (Xu et al., 2020; Klar, 2018) and soil heave (Palmer & Williams, 2003; Hawlader et al., 2006; Chaudhuri & Choudhury, 2022). These analytical methods are usually established based on the beam-on-elastic-foundation theory (Hetényi & Hetbenyi, 1946). In longitudinal analysis, the area of interest is the pipe buckling or tensile failure induced by longitudinal pipe-soil relative displacement (O'Rourke et al., 1995; Wham & Davis, 2019). Besides, analytical methods have been proposed to study the performance of jointed pipes, such as in cases of ground settlement (Klar, 2022) and longitudinal pipe-soil relative displacement (Wham & Davis, 2019).

The wide variety of such applications demonstrates the importance and popularity of analytical methods in evaluating the pipe-soil interactions of buried water pipes. However, it is laborious for a researcher that is new to this area to find relevant works from numerous sources, as such summary seems to be absent in existing literature which introduces the recent research developments and discusses possible future research directions. Xu et al. (2021) reviewed the dynamic responses of buried pipes, while only a small portion of the nine topics focused on analytical methods. Li et al. (2019) and Li et al. (2021) reviewed the interactions between pipes and frozen soils only. Tsinidis et al. (2019) reviewed the vulnerability of pipelines subject to seismic wave propagation without including other types of ground displacements.

This review article can help geotechnical researchers and engineers that are new to PSI studies using analytical methods have easy access to relevant works and build comprehensive awareness of the progress in the area. Through this work, the understanding of pipe performance under various scenarios can be enhanced. Features and limitations of each reviewed soil reaction model are discussed. To achieve the above goals, this work presents a thorough review of existing literature about analytical methods for studying pipe-soil interactions of buried water pipes in terms of cross-sectional, transverse and longitudinal directions. Offshore pipes that are not commonly used to transport water are out of the scope of this work. The structure of this paper is outlined as follows. First, the research methods are introduced in Section 2. Then, the scientometric analysis is performed in Section 3 discussing selected source journals, author contributions and keywords mapping. In Section 4, analytical methods studying cross-sectional, transverse and longitudinal PSI problems are discussed in detail. Then, Section 5 discusses possible future research trends in these fields based on the reviewed articles, followed by Section 6 which summarizes this work.

2 Research methods

The research methodology adopted in this work contains two consecutive phases: (1) scientometric analysis and (2) qualitative analysis. The former aims to familiarize the readers with authors and papers that contribute most to the analytical methods studying PSI. The latter technically reviews all papers collected in this work and discusses the current research gaps and future research directions. The procedures for conducting scientometric analysis generally follow those discussed in Tariq et al. (2021) and are briefly introduced below in this section. Figure 1 illustrates the research methods and sequences of this review paper.

First, the scientometric analysis was initiated by a preliminary validation through searching relevant keywords in Google Scholar and quickly going through the abstracts, main contents and conclusions of the papers. The searched keywords were "analytical" and "pipe-soil interaction" (or its synonyms such as "soil-pipe interaction"). This procedure was to design a broad framework for this review work and to make sure no similar review papers have been published. Second, screening criteria of including or abandoning a candidate paper were made. This was dependent on the scope of the sponsor project and the focus of studies that were found from online resources. The papers were included in this review if they focused on analytical methods studying PSI problems in cross-sectional, transverse and longitudinal pipe performance. On the other hand, they were abandoned if they focused on experimental or numerical methods, studied structure-soil interactions other than pipes, studied offshore pipes buried at sea level or written in non-English language. The purpose of this procedure was to ascertain that the topics of the collected papers agreed with the focus of this review. Third, papers were collected through searching the above keywords in Google Scholar and academic databases such as Scopus and Web of Science, as suggested by Tawfik et al. (2019), to enhance the accuracy and comprehensiveness of search

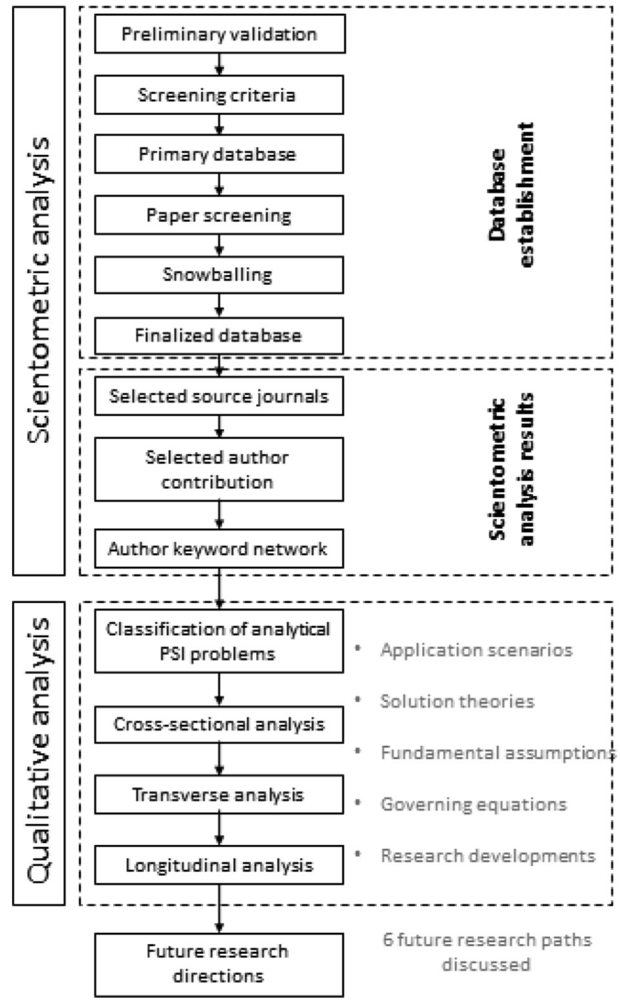

Fig. 1. Research methods and review structures.

results. A primary database was established including the titles, authors, publication years, source journals, author keywords, affiliations, references, citation reports, etc. Some of the papers were screened out and abandoned according to the above mentioned criteria through a quick examination of the keywords, abstracts and introduction part, while the main text of some papers were fully read to ascertain whether it is appropriate to be collected and what topic it is focused on. After this procedure, the size of collection was reduced from over 200 to 67 without duplication. Fourth, the rest of the papers were checked in terms of their references and cited-by data. This procedure, herein called "snowballing", was to include additional papers that were not found in previous procedures to build a more thorough collection of papers for subsequent scientometric analysis and qualitative analysis. For example, if a paper titled '*A*' was deemed relevant to the topic of this review and was collected through the above procedures, the papers that cite '*A*' as reference and the papers that are cited by '*A*' were collected as well, to enhance the adequacy of the number of papers collected for scientometric analysis and review. Furthermore, a new round of screening through reading the full text, especially the technical part, was performed to ensure these additional papers were relevant to the topics and met the criteria. By such, a total of 98 papers were collected in the finalized database. Science mapping analysis was then conducted using the VOSViewer (van Eck & Waltman, 2010). The results of scientometric analysis include summaries of selected source journals, author contribution and science mapping of author keyword network.

The second phase, qualitative analysis, was performed to systematically review the papers in the finalized database in terms of the application scenarios, solution theories, fundamental assumptions, governing equations and research developments. The classes of analytical methods studying PSI problems were cross-sectional, transverse and longitudinal. Research gaps were discussed, based on which six possible future research directions were presented.

3 Science mapping results

Discussions on science mapping results were classified as source journals, author occurrence and network of author-provided keywords. The results of science mapping provide summarized information of common journals that publish the relevant works, authors whose research focus is analytical methods for PSI studies and what keywords to search in academic resources. Table 1 shows some common journals in alphabetical order that publish studies on the analytical solution of PSI problems. 9 journals out of 33 were listed in Table 1. The readers can directly search these journals to access those research articles studying PSI problems with analytical methods. Some journals have a specific area of focus, for example, "Soil Dynamics and Earthquake Engineering" usually publishes relevant papers that investigate the performance of a pipeline crossing seismic faults, and "Tunnelling and Underground Space Technologies" tends to publish solutions of pipelines subject to ground settlement induced by tunnelling. On the other hand, some journals investigate multiple scenarios of pipeline performance. These journals are usually geotechnics-related, such as "Canadian Geotechnical Journal", "Computers and Geotechnics", "Geotechnique", "Journal of Geotechnical and Geoenvironmental Engineering" and "Soils and Foundations".

Table 2 lists selected authors in alphabetical order with their number of works that are cited in this review. The purpose of Table 2 is to allow readers to quickly be aware of the research experience of each author and access the relevant works. It also includes the authors' affiliations and the field of study of these papers. These study areas covered the three categories of review: cross-sectional, transverse and longitudinal with focuses on pipe cross-sectional ovalization, seismic fault crossing, pipe performance subjected to ground settlement, upheave and longitudinal pipe-soil relative displacement. Multiple soil reaction models and research focus have been studied. These areas, including those not listed in Table 2, are discussed in detail in Section 4.

Table 1
Selected source journals (in alphabetical order) that are collected in this review.

Source journals	No. of papers cited	Field of study
Canadian Geotechnical Journal	12	Ground settlement Jointed pipe Longitudinal displacement Seismic fault
Computers and Geotechnics	4	Ground settlement Upheave Weak soil
Geotechnique	7	Ground settlement Seismic fault Upheave
Journal of Geotechnical and Geoenvironmental Engineering	4	Ground settlement Jointed pipes
Journal of Pipeline Systems Engineering and Practice	4	Jointed pipe Upheave Longitudinal displacement
Journal of Transportation Engineering	8	Cross-sectional ovalization Longitudinal displacement
Soil Dynamics and Earthquake Engineering	13	Seismic fault
Soils and Foundations	4	Ground settlement Jointed pipe Fragility analysis
Tunnelling and Underground Space Technology	9	Ground settlement

Figure 2 shows the networks of author keywords in the collected database compiled through fractional counting by VOSViewer. In the network, the minimum number of occurrences of a keyword was set at 2, and 46 out of 243 keywords met this criterion. To avoid distraction, some synonyms were combined into one. For example, "pipe", "pipes" and "pipelines" were represented by "pipeline"; "soil-pipe interaction" and "pipe-soil interaction" were combined as "pipe-soil interaction"; "analytical solution" and "analytical model" were replaced by "analytical method". "Finite element method" or the abbreviation "FEM" were combined into "Finite element analysis". Keywords that occurred frequently were represented by larger nodes and stood in the center of Fig. 2. For example, "pipeline", "pipe-soil interaction" and "analytical method" are the largest nodes and occupy the cores of the network. "Finite element analysis" is also a large node because the analytical studies that are cited in this work are usually validated through comparison with numerical results. The outer keywords with small nodes represent the specific field of study using analytical methods. For example, "normal fault" and "ground settlement" are two keywords that explicitly indicate the focus of the respective works. This suggests that one can search these keywords to find the relevant articles that study pipe-soil interactions analytically. Such mapping of keywords analysis may be beneficial for potential authors to reach broader attention and find more areas

Table 2
Selected authors (in alphabetical order) that are cited in this review.

Author	Affiliation	No. of papers cited	Field of study
Cherniy V. P.	Research Institute for Natural Gases and Gas Technologies, Russia	3	Seismic fault
Huang M. S.	Tongji University, China	6	Ground settlement
Karamanos S. A.	University of Thessaly, Greece	4	Seismic fault
Karamitros D. K.	University of Bristol,UK	3	Seismic fault
Klar A.	Israel Institute of Technology, Israel	5	Ground settlement
Kouretzis G. P.	University of Newcastle, Australia	4	Seismic fault Ground settlement Upheave
Masada T.	Ohio University, US	5	Cross-sectional ovalization
Moore I. D.	Queen's university, Canada	7	Seismic fault Ground settlement Jointed pipe
Ni P. P.	Sun Yat-sen University, China	11	Seismic fault Ground settlement Jointed pipe Fragility analysis
Qin X. G.	Sun Yat-Sen University, China	5	Seismic fault Jointed pipe
Sargand S. M.	Ohio University, US	4	Cross-sectional ovalization
Soga K.	University of California, Berkeley, US	4	Ground settlement Upheave
Trifonov O.V.	Research Institute for Natural Gases and Gas Technologies, Russia	4	Seismic fault
Wang Y.	City University of Hong Kong, China	6	Seismic fault Ground settlement
Wham B. P.	University of Colorado Boulder, US	2	Longitudinal displacement
Yu J.	Tongji University, China	4	Ground settlement

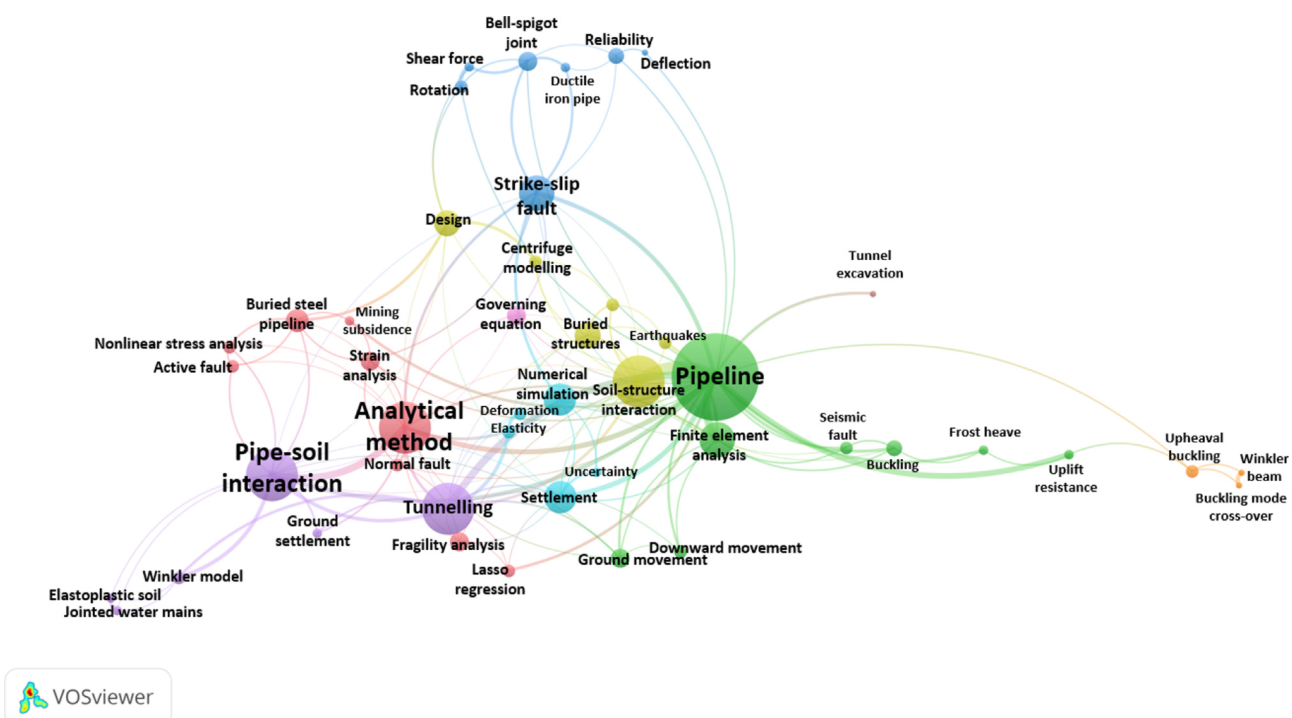

Fig. 2. Network analysis of author keywords.

of interest. It should be noted that some keywords are not directly linked to "analytical method", such as "upheaval buckling", while this does not mean analytical methods have not been applied to studying upheaval buckling of pipes. It is more likely because that the authors used a keyword that can more specifically describe the analytical method, like the Winkler beam (Gantes & Melissianos, 2014; Melissianos & Gantes, 2016).

4 Qualitative analysis

This section discusses the qualitative analysis of analytical methods studying PSI problems, which are classified into cross-sectional analysis (Section 4.1), transverse PSI (Section 4.2) and longitudinal PSI (Section 4.3). In Section 4.1, the analysis is classified into cross-sectional ovalization and circumferential deformation. In Section 4.2, the review follows the order of seismic fault (Section 4.2.1), weak soil zones (Section 4.2.2), ground settlement (Section 4.2.3) and pipe uplift (Section 4.2.4). In Section 4.2.1, Section 4.2.3 and Section 4.3 the review is performed separately for continuous and jointed pipelines because of their different failure modes, while in other sections the analysis focuses on continuous pipelines.

4.1 Cross-sectional analysis

Buried pipes can be classified as rigid, semi-flexible, flexible and compressible depending on the stiffness of the pipe materials relative to the surrounding soil stiffness (Moore, 2001). Rigid pipes carry vertical soil loads by their own stiffness, while flexible pipes sustain the applied loads by the combined effect of pipe stiffness and the horizontal thrusts. In this part, cross-sectional ovalization of flexible pipes and circumferential stress and strain induced by soil loads were discussed.

4.1.1 Ovalization

In the cross-sectional analysis of buried flexible pipes, the famous Iowa approach has been implemented for decades since it was first proposed by Spangler and Shafer (1938). Some Codes of Practice in pipeline or waterworks such as ALA (2001) directly adopt this methodology to compute the cross-sectional ovality. Later, Watkins and Spangler (1958) revised the original one and proposed the following modified equation:

$$\frac{\Delta x}{D} = \frac{0.5 D_{\mathrm{L}} K W_{\mathrm{c}}/r}{EI/r^3 + 0.061E'}, \tag{1}$$

where Δx is the horizontal change of pipe diameter, D is the outer diameter of the pipe, D_{L} is the time lag factor which accounts for continuing deflection of pipe with time, W_{c} is the vertical load on pipe crown exerted by soil fill, r is the original radius of the pipe, K is the dimensionless bedding constant depending on the bedding angle α (refer to Fig. 3), EI is the flexural rigidity of the pipe cross-section and E' is the modulus of soil reaction.

Figure 3 presents the hypothesis of the fill-load theory of the Iowa formula, which consists of the following three elements (Masada, 2000):

- The vertical load carried by a flexible pipe is determined by Marston's theory (Marston, 1930), and is approximately uniformly distributed over the pipe diameter. Marston's theory assumes that vertical loads are partly carried by the frictional forces along the trench wall and that the cohesion of soils is ignored. Moser and Folkman (2008) commented that the differential settlement between the backfill and the natural soil affects the amount of load carried by a pipe, while this is neglected in the traditional Iowa approach (but will be discussed later). The vertical load W_{c} in Eq. (1) carried by a flexible pipe, may be computed by $W_{\mathrm{c}} = C_{\mathrm{d}}\gamma BD$, where C_{d} is the load coefficient, γ is the unit weight of soil backfill and B is the trench width.
- The vertical reaction at the pipe bottom is uniformly distributed over the bedding (angle θ in Fig. 3) and equals the vertical load exerted on the pipe.
- The distribution of the passive horizontal pressure on both sides of the pipe is parabolic and is symmetric about the pipe's springline. The spanning of horizontal pressure is 100° and the maximum horizontal pressure $h_{\max} = e(\Delta x/2)$, where e is the modulus of passive soil resistance.

The parameters in Eq. (1) are readily available, except the modulus of soil reaction E' whose determination is usually indirect through the approximate one-to-one correspondence between one-dimensional constrained modulus M_{s} and E' (Hartley & Duncan, 1987). Equation (1) also holds the strength that it is supported by a vast database of flexible pipes. In recent years its application has also been extended to scenarios other than estimating horizontal deflections.

A direct extension of implementing the Iowa approach was the estimation of vertical deflections (Δz) of the pipes. In practice it was usually assumed that the Δz approximately equals to Δx, while it was found that Δz should be greater than Δx (Moser, 1994; Masada, 1996). Masada (2000) derived an analytical solution for the vertical deflection of flexible pipes based on the same assumptions as Eq. (1), and is shown as

$$\frac{\Delta z}{D} = \frac{P}{M_{\mathrm{s}}} \frac{KM_{\mathrm{s}}}{(EI/r^3)} \left(\frac{0.0595 M_{\mathrm{s}}}{(EI/r^3) + 0.061 M_{\mathrm{s}}} - 1 \right), \tag{2}$$

where $P = W_{\mathrm{c}}/(2r)$ is the vertical pressure on the pipe (refer to Fig. 3) and E' is substituted by M_{s} as explained above. The deflection ratio is approximated as

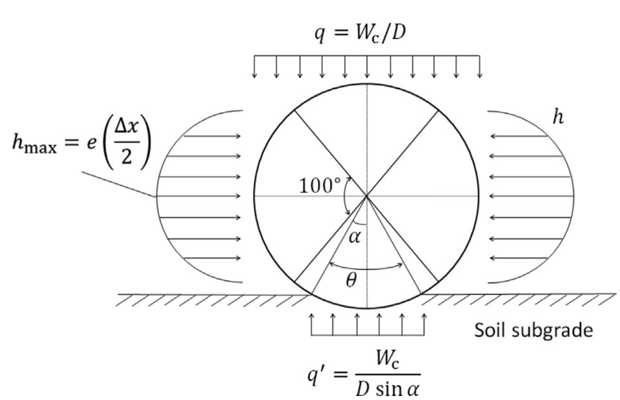

Fig. 3. Stress distribution hypothesis of Iowa formula.

$$\left|\frac{\Delta z}{\Delta x}\right| \approx 1 + \frac{0.0094E'}{\text{PS}}, \tag{3}$$

where PS is the pipe stiffness and is given by $EI/(0.149r^3)$. Equation (3) supports that the vertical deflections should be greater than the horizontal, and testing results demonstrated the efficacy of this equation. The percentage errors between measured (data extracted from Spangler & Shafer (1938)) and estimated deflection ratio were from 0.2% to 4.4% and 9.7% to 14.3% for the tamped and untamped backfill conditions, respectively. Parametric studies found that the increase of E' reduces both Δx and Δz nonlinearly, while increases the deflection ratio almost linearly. Increase in pipe stiffness has a negligible influence on Δx, but reduces Δz nonlinearly.

The above equations estimate pipe ovality over a relatively long time where pipe deforms into a horizontal ellipse under loads of native soil backfill, as shown in Fig. 4(a). However, deflection of pipes during initial backfilling could be in the shape of a vertical ellipse shown in Fig. 4(b), resulting from the horizontal forces generated by compactor and trench fill. This vertical elliptical deflection was termed 'peaking deflection' and was analytically studied by Masada and Sargand (2007). Denoting outward deflection being positive, the horizontal shortening induced by peaking deflection is expressed as

$$\frac{\Delta x}{D} = -\frac{(4.7P_{\text{c}} + K_0 r\gamma)}{3.874\text{PS}}, \tag{4}$$

where the numerator represents the horizontal soil pressure induced by (a) soil compaction P_{c}, which is dependent on soil type and compactor type, and (b) at-rest horizontal soil pressure K_0. Compared to the field measurement data reported by Sargand (2002), Eq. (4) estimated the peaking deflections relatively accurately for both polyvinyl chloride (PVC) and high-density polyethylene (HDPE) pipes under multiple backfill conditions. Masada and Sargand (2007) suggested that the peaking and long-term deflections may be superimposed to reach a possibly more realistic deflection estimation for buried flexible pipes.

As mentioned above, the traditional Iowa approach did not take into account the effect of differential settlement on the pipe vertical load. For a rigid pipe buried in a trench, sidefill soil settles more than the soil prism above the pipe and drags the pipe downward through frictional forces. This leads to a more significant vertical load on the pipe crown than the self-weight of the soil prism, which is termed negative soil arch effect. On the contrary, flexible pipes carry less load than the self-weight of the soil prism, which is termed positive soil arch effect. These two opposite effects are illustrated in Fig. 5. Besides, buried pipes may also suffer circumferential shortening, which contributes to the vertical deflection of a pipe as much as 15% for a HDPE pipe (Sargand & Masada, 2003). Therefore, positive soil arching and circumferential shortening effects should be both taken into account for calculating the deflections of a flexible pipe.

In this regard, Sargand et al. (2005) developed the modified Iowa formula by introducing a vertical arching factor (F_{va}). The improved formula is given by

$$\frac{\Delta x}{D} = \frac{D_L K P_{\text{va}}}{0.149\text{PS} + 0.061E'} - \frac{P_{\text{va}}}{E'}\left(\frac{0.364S_{\text{H}} + 0.061S_{\text{B}} + 0.012S_{\text{H}}S_{\text{B}}}{2.571 + 0.572S_{\text{H}} + 0.163S_{\text{B}} + 0.039S_{\text{H}}S_{\text{B}}}\right), \tag{5a}$$

$$F_{\text{va}} = 1 - 0.714\left(\frac{S_{\text{H}} - 0.7}{S_{\text{H}} + 1.75}\right) + 0.29\left(\frac{27.31 - S_{\text{B}}}{16.81 + S_{\text{B}}}\right), \tag{5b}$$

$$P_{\text{va}} = F_{\text{va}}\gamma H, \tag{5c}$$

where P_{va} is the vertical pressure on the pipe accounting for vertical arching effect, A is the cross-sectional area of the pipe, H is the height of soil fill above pipe crown (refer to Fig. 5), S_{B} and S_{H} are the bending stiffness parameter and hoop stiffness parameter, respectively. Field measurements of large-diameter HDPE pipes conducted by Sargand et al. (2005) revealed that the degree of soil arching (ratio of the measured soil pressure at pipe crown to the estimation through self-weight of soil backfill) varied in the range of 34% to 57%, and that the arching effect was more significant when the backfill soil was compacted denser or the particles of the backfill soils were larger and more angular. It was demonstrated that Eq. (5a) which includes soil arching effect and circumferential shortening better estimated the horizontal deflections of deeply buried flexible pipes than Eq. (1).

Despite the simple form and broad engineering applications of the modified Iowa formula (Eq. (1)), there still lacks a systematic study and sound understanding of the modulus of soil reaction E'. E' is not a real soil property. Rather, it is a parameter of pipe-soil interacting system. Its empirical nature implies that it can be acquired only through back calculating the field data with the buried pipe. Jeyapalan and Watkins (2004) carefully reviewed the E' values in the database of Howard (1977) and found that the percentage errors ranged from −944% to 491%. Sivakumar et al. (2006) conducted a reliability analysis which revealed that the coefficients of variation of E' significantly affected the reliability of pipe. Because of this, special caution should be paid for the choice of the E' values. Jeyapalan and Watkins (2004) provided a guideline of determining E' for design engineers based on the review of literature and their project experience. In the procedure, they introduced the ideas from Leonhard (1973) and Richard (2000) that E' can be expressed as

$$E' = S_{\text{c}}E'_{\text{b}}, \tag{6}$$

where S_{c} is the soil support combining factor and E'_{b} is the modulus of soil reaction of the pipe zone-backfill embedment. S_{c} can be determined based on the ratio of trench width to pipe diameter (B_{d}/D) together with the ratio of modulus of soil reaction of the natural soil to that of the backfill embedment ($E'_{\text{n}}/E'_{\text{b}}$), while E'_{b} is dependent on the

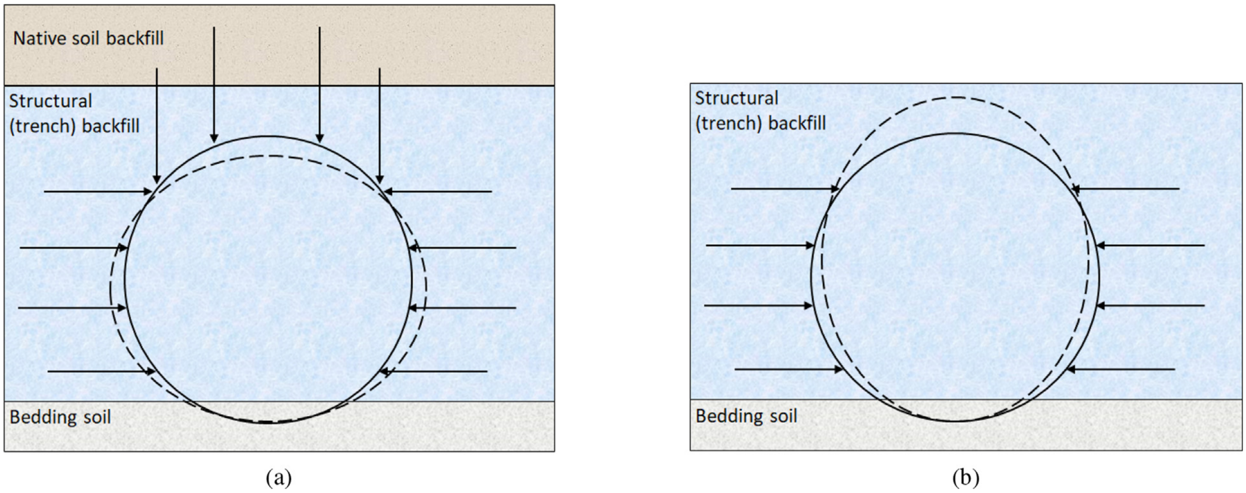

Fig. 4. (a) Long-term pipe deflection, and (b) peaking deflection.

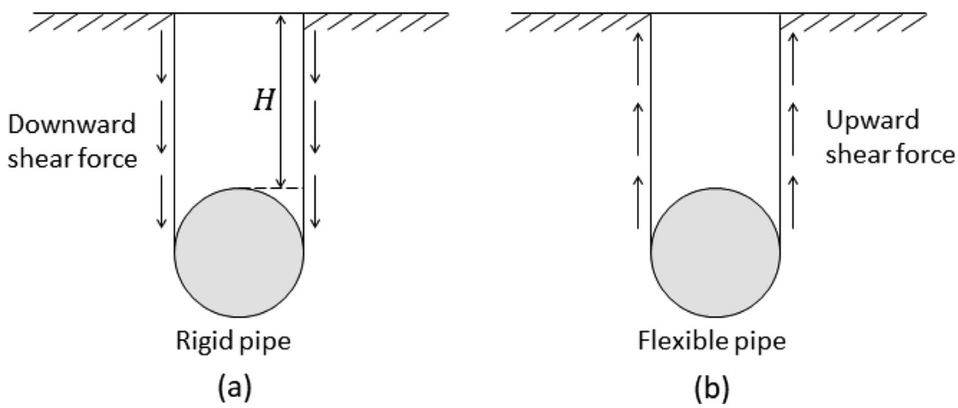

Fig. 5. Soil arch effect. (a) Negative soil arch over a rigid pipe, and (b) positive soil arch over a flexible pipe.

type of soil and the relative compaction density of the backfill. Coarser particles and higher density correspond to greater E'_b values. Compared to the method proposed in Hartley and Duncan (1987) which investigates the E' values based on the constrained soil modulus M_s with varying burial depth, the method by Jeyapalan and Watkins (2004) does not require assessing M_s, but it takes into account of the influence of trench width and the modulus of backfill soil. The methods of determining E' proposed by Hartley and Duncan (1987) and Jeyapalan and Watkins (2004) apply to flexible pipe buried in a trench, while whether the method is feasible for rigid pipes remains to be investigated. The values of both factors (S_c and E'_b) and the detailed calculating procedures can be referred to the tables in Jeyapalan and Watkins (2004) and Bowles et al. (2019).

4.1.2 Circumferential PSI

Rajani and Tesfamariam (2004) established analytical formulations of circumferential (hoop) stress and strain of a pipe subject to the combining effects of overburden load, internal pressure and external pressure, Poisson's effect from axial stress and temperature difference. The hoop stress σ_θ is composed of the following:

$$\sigma_\theta = \sigma_\theta^{\mathrm{w}} + \sigma_\theta^{\mathrm{P}} + \sigma_\theta^{\mathrm{T}} + \sigma_\theta^{\mathrm{a}}, \tag{7}$$

where $\sigma_\theta^{\mathrm{w}}$ is the hoop stress induced by the overburden load, $\sigma_\theta^{\mathrm{P}}$ induced by the internal and external pressure, $\sigma_\theta^{\mathrm{T}}$ induced by the thermal gradient between inside of a pipe and ambient soil and σ_θ induced by the axial stress. This formulation was made based on the assumption that the pipe is rigid and that the lateral earth pressure K_0 is zero. These assumptions were deemed appropriate and conservative for typical sizes of water mains. It was shown that σ_θ^T could reach over 14 MPa in a 6-inch diameter cast-iron pipe with a 10°C temperature change. Trifonov and Cherniy (2012) and Zhang et al. (2017) established elasto-plastic hoop stress and strain with the Von-Mises yield criterion. Unfortunately, it seems these formulations were not validated against any numerical or experimental evidence.

4.2 Transverse PSI

Permanent ground displacements (PGD) that are transverse to the pipe longitudinal axis may cause great damage to buried pipelines. Transverse pipe displacements can be induced by surface loads (Wang & Moore, 2014, 2015), seismic faults (Karamitros et al., 2007; Trifonov & Cherniy, 2010), landslides (Chaudhuri & Choudhury, 2020; Cocchetti et al., 2009), ground settlement (Iimura, 2004; Klar et al., 2005), loss of soil support due to weak zones (Rajani & Tesfamariam, 2004; Imanzadeh et al., 2013) and soil upheave (Singh et al., 2020; Nixon & Oswell, 2010). Since pipelines subject to surface loads, seismic fault and landslides can be studied using similar analytical approach and the principal difference is from the ground movement profile, this review discusses the studies on pipelines crossing seismic faults only as the relevant articles are more ample. Design of thrust restraint at pipe bends can also be studied with transverse PSI (Liu & Ortega, 2021), but the source is very limited and is not included here. This part discusses the flexural behaviour of pipes subject to transverse PGD.

4.2.1 Seismic faults

Seismic faults are geological discontinuity caused by earthquakes where continuous soil or rock mass shifts over another, forming a fault plane between the two blocks. Figure 6 shows three major types of seismic faults. If a fault plane is inclined, the block over the plane is the hanging wall and the block below the plane is the foot wall. A normal fault is formed when the hanging wall shifts downward relative to the foot wall, while a reverse fault is formed vice versa. A strike-slip fault is formed when the two blocks shift horizontally relative to each other. Since joints which connect pipe segments bring further complexity to the solutions of pipe performance, the review is performed separately for continuous and jointed pipes in this part. The focus is put on the continuous pipelines as the analysis also forms the basis of jointed pipes.

Continuous pipelines. In PSI problems where pipes are subject to seismic faults, it has been a popular method to consider the long pipeline as a cable (Newmark & Hall, 1975; Kennedy et al., 1977) rested on soil foundations. However, cables cannot sustain flexural stresses and the method did not take into account the stiffness of a pipe in resisting transverse PGD. Then Wang and Yeh (1985) modelled the pipe as a beam with bending stiffness. The method partitioned the pipe into segments where the ones close to the fault were assumed to be circular arcs while those far from the fault were treated as beam-on-elastic-foundation. The beam-on-elastic-foundation method is sometimes associated with the Winkler model where a beam is supported by a system of discrete, mutually independent elastic soil springs. Karamitros et al. (2007) further refined the method by assuming the segments close to the fault as an elastic beam. The theories of elastic-beam and beam-on-elastic-foundation form the basis for analytical solutions of the pipeline crossing seismic faults. Equation (8) is the governing equation of beam-on-elastic-foundation theory. EI has the same meaning as in Eq. (1), $w(x)$ is the transverse displacement of the pipe along its longitudinal axis and k_s^t is the transverse spring stiffness of the elastic soil foundation. Equation (8) is also the governing equation of elastic-beam theory if $k_s^t w(x)$ is replaced by a distributed load q. It should be noted that Eq. (8) is only valid for Euler–Bernoulli beam theory that assumes all plane sections remain plane and are perpendicular to the neutral axis of the beam. It is applied to analyzing the bending-induced deflections and stresses of thin structures, which suits analytical calculations of pipeline crossing a strike-slip fault or normal fault (Ghavami, 2014). Though more complex beam theories are available, for example, the Timoshenko beam theory which takes into account of the influence of shear forces on deflections, they are out of the scope for analyzing bending-induced pipeline behaviours (Timoshenko & Goodier, 1951). Figure 7 illustrates these parameters and the deflection of a pipe.

$$EI\frac{\mathrm{d}^4 w}{\mathrm{d}x^4} + k_s^t w(x) = 0, \tag{8}$$

Vesić (1961) derived a solution for k_s^t as

$$k_s^t = \frac{0.65E_s}{1-\nu^2}\sqrt[12]{\frac{E_s D^4}{EI}}, \tag{9}$$

where ν is the Poisson's ratio and E_s is the elastic stiffness of soil foundation. First, second and third-order differentiation of w give the rotation angle θ, the bending moment M and the shear force V of the pipeline, respectively, as shown in Eq. (10a) to Eq. (10c).

$$\tan\theta = \frac{\mathrm{d}w}{\mathrm{d}x}, \tag{10a}$$

$$M = -EI\frac{\mathrm{d}^2 w}{\mathrm{d}x^2}, \tag{10b}$$

$$V = -EI\frac{\mathrm{d}^3 w}{\mathrm{d}x^3}. \tag{10c}$$

The general solution of Eq. (8) is

$$w(x) = \mathrm{e}^{\lambda_s^t x}\left(c_1 \sin\lambda_s^t x + c_2\cos\lambda_s^t x\right) + \mathrm{e}^{-\lambda_s^t x}\left(c_3\sin\lambda_s^t x + c_4\cos\lambda_s^t x\right), \tag{11}$$

where $\lambda_s^t = \sqrt[4]{\frac{k_s^t}{4EI}}$ and c_1 to c_4 are constants to be determined from boundary conditions. With these, analytical solutions of flexural performance of a pipeline crossing faults are available. The hypothesis and theories adopted in Karamitros et al. (2007) were

- The pipeline crossing the fault is partitioned into four parts, which are segmented by Point A, B and C in Fig. 8. Point A and C are supposed to be the points closest to B without lateral displacement.
- The fault plane has a zero thickness so Point B represents the intersection of the pipeline and the fault plane.
- The geometry shown in Fig. 8 is anti-symmetric about B and the computation can be performed on one side of the fault plane (A'B).

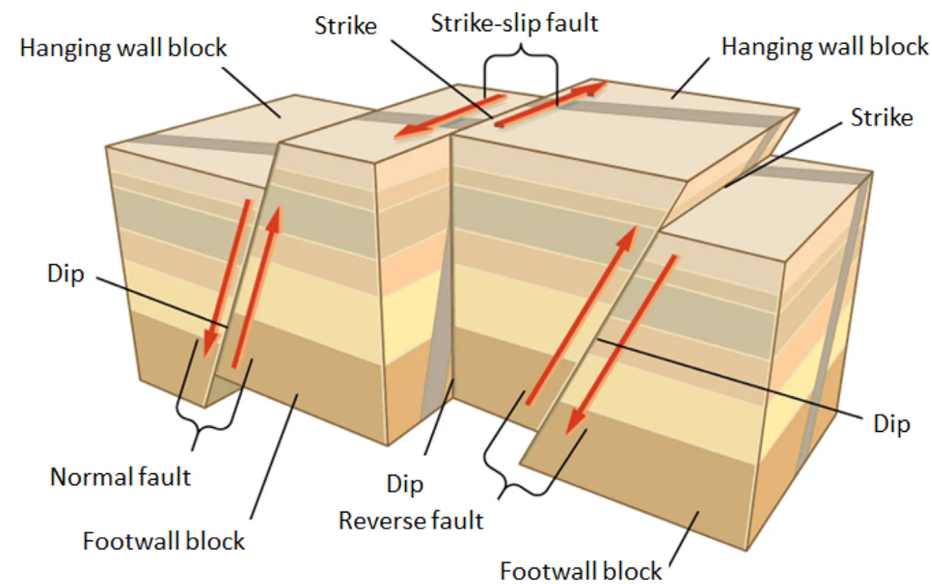

Fig. 6. Types of seismic faults (Britannica, The Editors of Encyclopedia, 2022). (By courtesy of Encyclopedia Britannica, Inc., copyright 2016; used with permission).

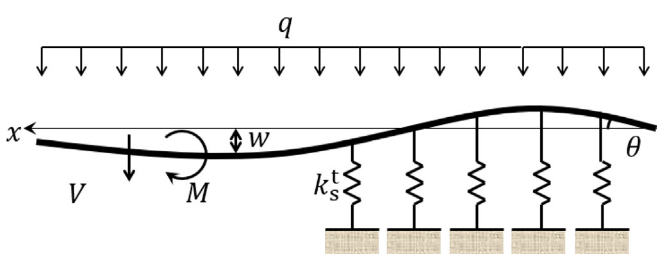

Fig. 7. Schematic illustration of beam method.

- The lateral loads q on the pipe imposed by relative pipe-soil displacement are uniform and can be estimated according to ALA (2001).
- The transverse fault displacement Δy in Fig. 8 does not contribute to pipe elongation.
- The pipe displacement does not cause buckling.

An iterative approach was performed to derive the axial and bending stress and strain on the pipe, until the results converged. The procedure is encapsulated as below

1. Segment AA' is analyzed by beam-on-elastic-foundation theory. The boundary conditions assume that $w(x)$ at A and A' (far from Point A) are zero.
2. Segment AB is analyzed by elastic-beam theory with a rotational spring at A and a joint at B, through which the shear force and bending moments at A and B can be obtained together with the boundary conditions. Maximum bending moments in Segment AB can be derived as well.
3. The axial strain at B is computed indirectly from the compatibility of pipeline elongation induced by fault displacement and accumulated along the unanchored length. Tensile stress and strain are computed with a bilinear stress–strain response and the assumption of linear attenuation of axial stress away from the fault.
4. The maximum bending strain $\varepsilon_{b,max}$ is approximated as $\varepsilon_{b,max} = \frac{\varepsilon_b^I \varepsilon_b^{II}}{\varepsilon_b^I + \varepsilon_b^{II}}$, where ε_b^I is derived from elastic-beam theory and ε_b^{II} from second-order geometric effect (neglecting pipe bending stiffness).
5. The total strain in the pipe is obtained from adding the axial strain and bending strain in the cross-section ($\varepsilon = \varepsilon_b \cos\omega_c + \varepsilon_a$, where ω_c is the angle of the point of interest in the pipe cross-section).
6. The secant modulus of pipe material is updated according to the axial and bending strains, to account for the nonlinear behaviour and adopted in the next iteration.

Karamitros et al. (2007) validated their novel analytical approach by comparing the results against FEM simulations with pipe-fault intersection angle $\beta = 30^\circ, 45^\circ$ and 60°, and with a fault displacement $\Delta f \leq 2D$. Overall good agreements between the analytical and numerical results were observed in terms of axial strain at Point B, maximum axial strain, bending strain and maximum total strain, though for large fault displacements when $\Delta f \geqslant 1.5D$ the analytical method under-predicted these strains because Δy was assumed not to contribute to pipe elongation. Wang et al. (2011) replaced the bi-linear stress–strain relationship with the Ramberg–Osgood relationship (Ramberg & Osgood, 1943) to the analytical method. They confirmed the accuracy of the analytical method for $\Delta f \leq 10D$.

Karamitros et al. (2011) and Hu et al. (2022) omitted the anti-symmetry assumption and combined Segment AB and BC in Fig. 8 as one segment. This allows such analytical methods to be used in both strike-slip and normal fault crossings. Strains obtained from the method were com-

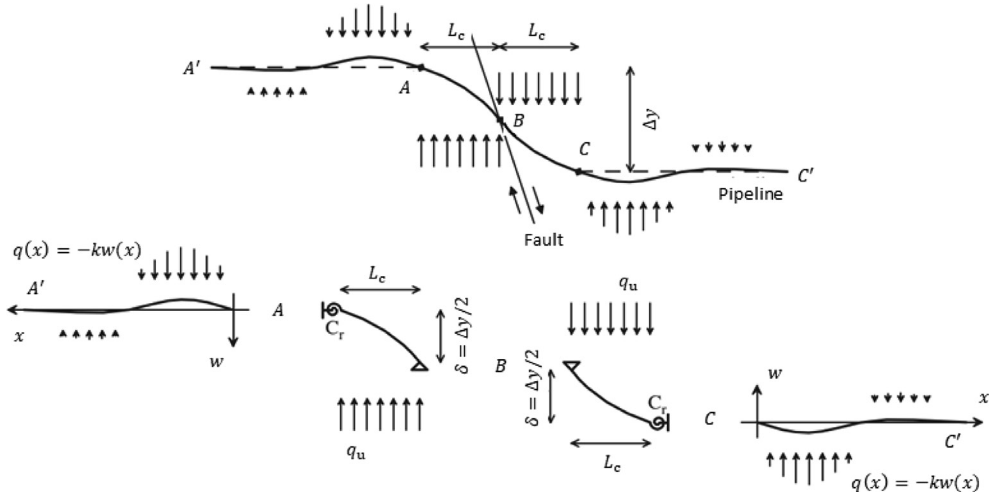

Fig. 8. Partitioning of a pipe crossing strike-slip faults, reproduced from Karamitros et al. (2007) with permission from Elsevier.

pared with FEM results for three cases of normal fault crossing, with intersection angle $\beta = 55^\circ, 70^\circ$ and 85°. Good agreements were observed for the first two cases. While the analytical method again under-predicted the strains when $\beta = 85^\circ$ and $\Delta f \geqslant 1.2D$, because of the reason discussed above. To remedy the discrepancy between analytical and FEM results when β is close to 90° or Δf is large, Trifonov and Cherniy (2010) took into account the contribution of transverse fault displacement to pipe axial elongation. Besides, the axial force term was directly incorporated into the governing equation in Segment AC as

$$EI\frac{\mathrm{d}^4w}{\mathrm{d}x^4} + F\frac{\mathrm{d}^2w}{\mathrm{d}x^2} + q = 0, \tag{12}$$

where F is the pipe axial force. This eliminated the defects of approximating bending strains in Karamitros et al. (2007) and was more physically rational. The results demonstrated the influence of transverse fault displacement on pipe elongation when $\Delta f \geqslant 1.2D$. Alternatively, Trifonov et al. (2011) modified pipe strain calculation by empirically introducing a stiffness reduction factor and two stiffness distribution factors. The former was dependent on the location of the maximum bending moment and the length of strain concentration. The latter was dependent on the maximum bending strain and the ratio of average to maximum bending strain $\varepsilon_{\mathrm{b,av}}/\varepsilon_{\mathrm{b,max}}$. This modification, although empirical, provided a closer match to FEM results in terms of maximum strains and bending strains, especially for $\beta \geqslant 80^\circ$ and $\Delta f \geqslant D$.

Apart from axial and bending induced by pipe crossing seismic faults, pipes also carry service loads such as internal pressure P_i and temperature difference ΔT (Trifonov, 2018). Trifonov and Cherniy (2012) attempted to take these into account in the analytical methods for a more thorough representation of pipe performance. These service loads were assumed constant in their analysis. Under plane stress conditions, the elastoplastic stress–strain relationship was adopted with the Von-Mises yield criterion. The elastic components of axial, hoop and radial strains were computed from generalized Hooks' law. The corresponding plastic strains were computed incrementally with the assumption of the associated flow rule and linear hardening of the yield surface. Thermal strains were assumed constant. Then the total strains were the sum of elastic, plastic and thermal components. Comparisons were made between analytical and FEM results with variations in pipe-fault intersection angle β, fault displacement Δf, temperature difference ΔT, hoop stress σ_θ and internal pressure P_i. General agreements were observed. A non-monotonic effect of P_i on the maximum total strain was evident. The rise in ΔT was found favorable in this case, where the tensile stress in the pipe resulting from fault crossing was partially compensated. Zhang et al. (2017) improved the accuracy of analytical results in estimating strains under large fault displacement. This was accomplished by omitting the assumption of constant axial force in Segment AB (Fig. 8) and dividing it into infinitesimal segments, each of which satisfied the force equilibrium in axial and transverse directions.

The analytical approach discussed so far did not implement axial PSI into the governing equations. Specifically, equations of pipe axial force F mobilized from longitudinal pipe-soil relative displacement were not established. Talebi and Kiyono (2020) introduced the governing equation of axial PSI based on a pipe segment subject to longitudinal fault split δ_x without relative pipe-soil sliding

$$EA\frac{\mathrm{d}^2u}{\mathrm{d}x^2} + k_\mathrm{s}^\mathrm{a}u(x) = 0, \tag{13}$$

where $u(x)$ is the pipe displacement along its longitudinal axis and k_s^a is the axial soil spring stiffness. The solution to Eq. (13) is

$$F_{\mathrm{f}}(x)=\frac{k_{\mathrm{s}}^{\mathrm{a}}\delta_x}{\lambda_{\mathrm{a}}}\mathrm{e}^{-\lambda_{\mathrm{a}}x},\tag{14}$$

where $F_{\mathrm{f}}(x)$ is the pipe axial force due to pipe-soil friction and $\lambda_{\mathrm{a}}=\sqrt{k_{\mathrm{s}}^{\mathrm{a}}/EA}$. The axial force $F_{\mathrm{m}}(x)$ due to geometrical nonlinearity (membrane force) in Segment AB can be expressed as

$$F_{\mathrm{m}}(x)=\frac{EA\cos\theta}{|L_{\mathrm{conv}}-x|}\int_x^{L_{\mathrm{conv}}}\left(\sqrt{1+\theta^2}-1\right)\mathrm{d}x,\tag{15}$$

where $\theta=\mathrm{d}w/\mathrm{d}x$ is the rotation of pipeline and L_{conv} is the length of the curved pipe from Point B to the far end A' (Fig. 8) where $w(x)$ is almost attenuated. The sum of $F_{\mathrm{f}}(x)$ and $F_{\mathrm{m}}(x)$ yields the total pipe axial force $F(x)$, which related M and V in the form of

$$\frac{\mathrm{d}M}{\mathrm{d}x}\approx F\frac{\mathrm{d}w}{\mathrm{d}x}+V.\tag{16}$$

Equation (16) gives the governing equation of Segment $A'B$ which takes axial force and geometrical nonlinearity into account. Solutions to Eq. (16) showed accurate agreements with FEM results in estimating the axial forces, bending moments, shear forces and maximum stresses under strike-slip faults with intersection angle β from 45° to 90° and fault displacement Δf from $1D$–$6D$. Based on the achievements in Talebi and Kiyono (2020, 2021) further extended the linear behaviour to the nonlinear behaviour of axial PSI. They established the equations of $F_{\mathrm{f}}(x)$ for both non-sliding and sliding cases. Besides, they omitted the assumption of pipeline partitioning adopted in most previous studies and used unified governing equations to represent the transverse PSI of the entire pipeline. The study examined the variations of axial force, shear force, bending moment, maximum stress on pipe springline and maximum stress on pipe crown, with a maximum distance of 20 m away from the pipe-fault intersection point. It was shown that the analytical results successfully matched with FEM results both qualitatively and quantitatively, except the axial forces at $\beta=90°$.

In the above studies, bending and tension were assumed to be dominant behaviours when a pipe crossed a seismic fault. However, this is incomplete because compression and local buckling may occur due to pipe bending. Neglecting the interactions between soil and pipe, Vazouras et al. (2010) proposed an analytical method to estimate the compressive strain in a deformed pipe and to evaluate the occurrence of local buckling. The method was proposed based on the assumptions that the fault plane was perpendicular to the pipe longitudinal axis (i.e., $\beta=90°$) and that the pipe deformed in a presumed S-shape function, as shown in Fig. 9, where Δf is the fault displacement and L_{S} is the projected length of the deformed pipe. The bending strain ε_{b} can be derived from the deformation function. The axial strain ε_{a} was assumed to be uniformly distributed. Moreover the corresponding compressive strain ε_{c} was calculated as the difference between ε_{b} and ε_{a}. These three strains can be expressed as

$$\varepsilon_{\mathrm{b}}=\left(\frac{\pi}{2L_{\mathrm{S}}}\right)^2D\Delta f,\tag{17a}$$

$$\varepsilon_{\mathrm{a}}\approx\left(\frac{\pi\Delta f}{4L_{\mathrm{S}}}\right)^2,\tag{17b}$$

$$\varepsilon_{\mathrm{c}}=\varepsilon_{\mathrm{b}}-\varepsilon_{\mathrm{a}}\approx\frac{\pi^2}{4L_{\mathrm{S}}^2}\left(D\Delta f-\frac{(\Delta f)^2}{4}\right).\tag{17c}$$

The maximum compressive strain $\varepsilon_{\mathrm{c,max}}$ was derived by differentiating Eq. (17c) as

$$\varepsilon_{\mathrm{c,max}}=\left(\frac{\pi D}{2L_{\mathrm{S}}}\right)^2.\tag{18}$$

Hu et al. (2022) adopted the presumed deformation method and distinguished the upward and downward soil resistance in examining the performance of a pipe crossing a normal fault. Soil behaviours were characterized using the Mohr–Coulomb elastoplastic model. Vazouras et al. (2012, 2015) extended the use of the analytical method to the cases where $\beta\le 90°$ and took into account the pipe axial elongation. Sarvanis and Karamanos (2017) further extended the method to be applied to asymmetric cases and proposed a method to determine the length of the deformed pipe segment L_{S}.

Paolucci et al. (2010) and Ni and Mangalathu (2018b) adopted the dissipated energy method to study the pipeline performance crossing a seismic fault. The method is featured by the assumption that plastic hinges are formed at both sides of the fault plane and the flexural deformation is concentrated at hinges. Figure 10 illustrates the failure mechanism of the pipe using this method, where the pipe segment between the two hinges undergoes plastic deformation. The method does not require presuming a deformation shape of the pipeline (c.f. Vazouras et al., 2010; Hu et al., 2022). Rather, it determines the deflected shape through the minimum energy dissipation theorem, where the only unknown geometrical quantity is the angle ϕ_{p}, as shown in Fig. 10. The total dissipated energy P_{r} due to infinitesimal increment of fault displacement $\mathrm{d}f$ in the PSI system, consists of four parts: (1) P_{r1}, the energy dissipated by rotation of plastic hinges, (2) P_{r2}, the energy dissipated by plastic elongation of the pipe segment between plastic hinges, (3) P_{r3}, the energy dissipated by longitudinal soil-pipe relative motion and (4) P_{r4}, the energy dissipated by transverse soil-pipe relative motion. The governing equations of the four energy components can be referred to Eq. (19a) to Eq. (19d)

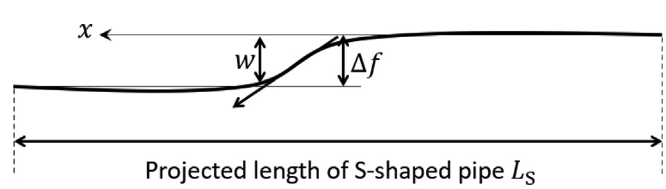

Fig. 9. Illustration of S-shape deformed pipe crossing a fault (fault plane is perpendicular to the pipe longitudinal axis).

$$P_{r1} = 2M_p\dot{\phi}_p, \tag{19a}$$

$$P_{r2} = F_p\dot{s}(x), \tag{19b}$$

$$P_{r3} = \int_0^{L_t} t_u(x)\dot{s}(x)\mathrm{d}x, \tag{19c}$$

$$P_{r4} = \int_0^{L_t} p_u(x)\dot{f}_t(x)\mathrm{d}x, \tag{19d}$$

where M_p is the plastic moment of pipe cross-section, $\dot{\phi}_p$ is the incremental change of ϕ_p per $\mathrm{d}f$, F_p denotes the longitudinal force in the plastic deformation range, $\dot{s}$ denotes the incremental change in pipe elongation in the plastic deformation range, L_t denotes the segment length, t_u denotes the limiting resistance force per unit length in the longitudinal direction due to soil-pipe relative motion, p_u denotes the limiting resistance force per unit length in the transverse direction due to soil-pipe relative motion and $\dot{f}_t$ is the transverse component of incremental fault displacement. M_p and F_p are available from analytical solutions of elastic-beam theory, t_u and p_u can be referred to empirical expressions (ALA, 2001), and $\dot{s}$ and $\dot{f}_t$ can be solved through geometric relationships. Thus, the four energy components can be solved against the fault displacement Δf, and the minimized P_r corresponds to the failure conditions. The accuracy of this method has been verified against numerical modelling results and other analytical methods.

Jointed pipelines. The flexural rigidity and shear resistance of joints are usually different from the pipe segments. Analytical solutions of continuous pipelines cannot be directly applied to jointed pipes since the stress and deformation are not differential at the joints. Besides, the failure modes of jointed pipe may be dominated by joint failures (e.g., bell split, joint shear failure and pull-out failure) instead of pipe bending failure (Rajani & Abdel-Akher, 2013; Qin & Wang, 2022). When a jointed pipeline crosses a seismic fault, the kinematics are different between an odd (the fault plane crosses at the joint) and an even (the fault plane crosses at the center of the pipe segment) condition, and the associated pipe performance is also different (O'Rourke & Liu, 2012). Therefore, a separate analysis of jointed pipeline performance is deemed appropriate for this part.

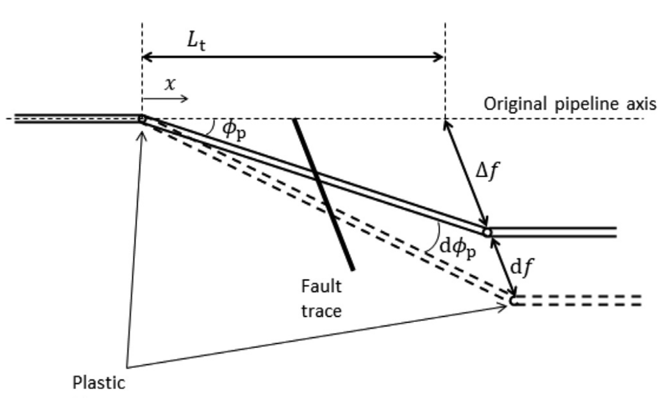

Fig. 10. Illustration for failure mechanism using energy dissipation method.

To study the performance of a jointed pipe subject to seismic fault crossing, it is usually assumed that the pipe segments between joints are simply supported beams on elastic foundations, where the joints do not carry moment resistance and serve as hinge supports (Valsamis & Bouckovalas, 2020; Qin et al., 2022). Qin et al. (2022) investigated the performance of a bell-spigot jointed pipe (a typical joint structure for water pipes) crosses a strike-slip fault using the beam method. Figure 11(a) illustrates the structure of a bell-spigot joint and the components of the beam-on-elastic-foundation analytical model, where the PSI elements consist of both transverse and axial components, and joint springs consist of axial, shear and rotational components. Then, the stresses and deformation of pipe segments, the rotation and shear forces of joints can be solved analytically through the elastic-beam theory, though the procedures are complex as the analytical model consists of multiple pipe segments and PSI components. Their study investigated the effect of relative position of the fault L_{rp} on the pipe performance, as illustrated in Fig. 11(b), where $L_{rp} = 0$ or 1 denotes an odd condition and $L_{rp} = 0.5$ denotes an even condition. It was found that an odd condition corresponds to the least joint rotation, but $L_{rp} \approx 0.3$ corresponds to the largest joint rotation for fault-crossing angle $\beta = 50^\circ$. The smallest axial translation occurs at $L_{rp} = 0.5$ (i.e., even conditions). Qin and Wang (2022) used the same approach to investigate the failure modes of bell-spigot joint pipes subject to fault crossing. They found that joint pull-out failure dominates when the pipe is buried shallow beneath the surface, while pipe bending failure controls when the pipe is buried deep. The worst fault crossing condition occurs at $L_{rp} \approx 0.1$ but not odd or even conditions.

4.2.2 Weak soil zones

A broken pipe may partially lose soil support when water leaks from the pipe and scours surrounding soil (Rajani & Tesfamariam, 2004). Plastic soil deformation could occur near the unsupported regions if the pipe overburden pressure is high or the unsupported length is large. Figure 12 shows a schematic illustration of partial loss of soil support. To accommodate the pipe responses in the plastic portion, Rajani and Tesfamariam (2004) defined an elastic limit deformation w_{lim} and a plastic transverse displacement w_p. The governing equations of the plastic and unsupported portions are given in Eq. (20a) and Eq. (20b), respectively

$$EI\frac{\mathrm{d}^4 w_p}{\mathrm{d}x^4} + k_s^t w_{lim} = 0, \tag{20a}$$

$$EI\frac{\mathrm{d}^4 w_u}{\mathrm{d}x^4} + q = 0. \tag{20b}$$

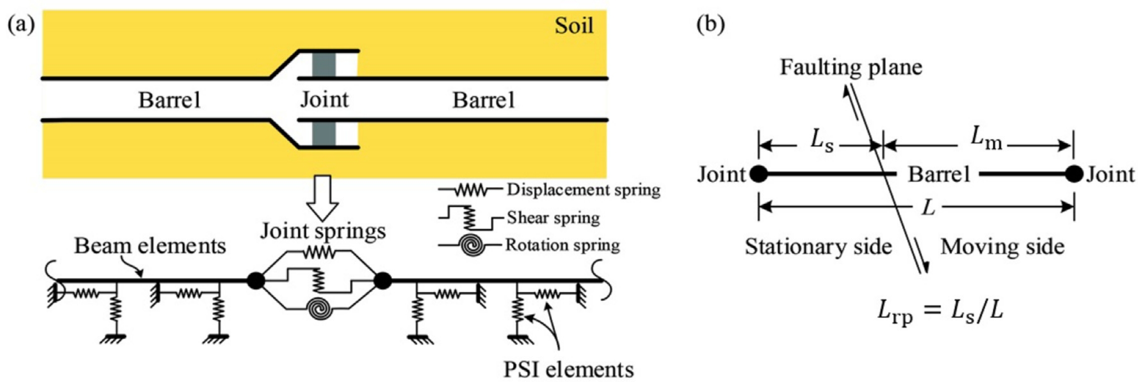

Fig. 11. Schematic illustration of a bell-spigot jointed pipe. (a) The structure of a bell-spigot joint connection and components of the beam-on-elastic-foundation analytical model, and (b) illustration of the relative position of fault L_{rp}, from Qin et al. (2022).

A sensitivity analysis was also performed by Rajani and Tesfamariam (2004) to investigate the influence of the length of unsupported region, pipe material properties and soil properties. It was found, as expected, that the longer the unsupported length is, the larger stress the pipe suffers. Metallic pipes can generally tolerate more loss of support than plastic pipes. The stress developed in pipes was highly dependent on the soil properties as well, i.e., maximum bending stress was more significant in pipes buried in weaker soils. Rajani and Tesfamariam (2004) did not take into consideration the strain limits which may differ for orders of magnitude for different materials. For example, the allowable strain limit is suggested to take as small as 0.02% for gray iron pipelines, while for profiled HDPE pipe or polyvinyl chloride (PVC) pipe the allowable strain can be 7.5% (Ni & Mangalathu, 2018a; Brachman et al., 2008). It is worth noticing whether the behaviour is ductile or brittle when the pipes are subject to lack of soil support.

Tesfamariam et al. (2006) cast the beam method into a possibilistic framework to investigate the influence of a bunch of parameters on the structural safety of the pipe. The influence of unsupported length and temperature difference was more pronounced on small-diameter pipes ($D = 150$ mm) than on large-diameter pipes ($D = 500$ mm). External loads triggered higher risks for large-diameter pipes than for small-diameter pipes. Similar work was performed by Shao and Zhang (2008) where they observed that weak soil, small pipe diameter, poor bedding support and large external loads were prone to causing plastic deformation. Imanzadeh et al. (2013, 2017) conducted an uncertainty analysis of the effects of soil and pipe parameters on the pipe performance. In the former, it was shown that the length of low stiffness zone had a more significant influence than the elastic modulus of soil foundation on the uncertainties of differential settlement and bending moment of a pipe. The latter collected data of soil properties from a real construction site. Results from the case study showed that spatial variability of the elastic modulus of the soil foundation (E_s) led to malfunction of a continuous pipe where the allowable counter slope was exceeded.

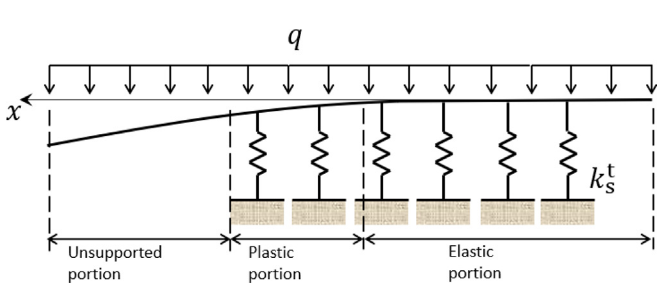

Fig. 12. Schematic illustration of weak soil support.

4.2.3 Ground settlement

Tunnelling or mining could induce extensive ground settlement, triggering vertical displacement and longitudinal deformation of buried pipes. The influence of ground settlement on pipe performance can be analytically studied using the beam-on-elastic-foundation method (Iimura, 2004; Klar et al., 2005; Wang et al., 2011; Kouretzis et al., 2015; Ieronymaki & Whittle, 2017; Xu et al., 2020) or elastic continuum method (Klar et al., 2005; Zhang et al., 2012; Klar, 2018, 2022; Lin & Huang, 2019). Both methods can be used to study continuous and jointed pipelines. The analysis of continuous and jointed pipelines is performed separately. The advantages and weaknesses of each modelling method are also discussed.

Continuous pipelines. The ground profile of a mining-induced ground settlement is usually assumed by a probability integral function (Xia & Zhang, 2017; Xu et al., 2020). Xia and Zhang (2017) studied the axial strain of pipeline under mining subsidence, through equating the pipe elongations induced by axial force and geometrical second-order effect. Xu et al. (2020) used the same method to examine the axial stress of pipelines subject to mining subsidence, and studied the pipe bending performance through the elastic-beam method. For tunnelling-induced ground settlement, it is popular to assume the ground profile as a Greenfield function (a Gaussian curve) $S_v(x)$ as

$$S_{\mathrm{v}}(x) = S_{\max} \mathrm{e}^{-\frac{1}{2}\left(\frac{x}{i}\right)^2}, \tag{21}$$

where $S_{\max}$ is the maximum settlement, x is the horizontal distance from a point on $S_{\mathrm{v}}(x)$ to the tunnel centerline and i is the horizontal distance of inflection point to the tunnel centerline. Sometimes a modified Gaussian curve is used to describe the soil settlement with greater accuracy (Vorster et al., 2005). Figure 13 shows schematically a pipeline perpendicularly crosses over a tunnel.

A common solution for analyzing pipeline performance due to tunnelling is the beam-on-elastic-foundation method (Klar et al., 2005; Wang et al., 2011; Huang et al., 2019). Its governing equation is similar with Eq. (8) except the right hand side is replaced by $k_{\mathrm{s}}^{\mathrm{t}} S_{\mathrm{v}}(x)$, as

$$EI \frac{\mathrm{d}^4 w}{\mathrm{d}x^4} + k_{\mathrm{s}}^{\mathrm{t}} w(x) = k_{\mathrm{s}}^{\mathrm{t}} S_{\mathrm{v}}(x). \tag{22}$$

The solution to Eq. (22) using Winkler model is usually associated with the Vesic's expression of the modulus $k_{\mathrm{s}}^{\mathrm{t}}$ (Eq. (9)). The Winkler model is a single-parameter model which assumes that the soil springs are closely spaced and mutually independent, and that the deflection of one spring will not induce deflection at another point. This restricts its application to non-cohesive soils where the interaction among adjacent soil elements is not significant (Wang et al., 2005). While in real circumstances a stress at a point can induce deflections at adjacent points through shear and soil behaves as a continuum medium.

Methods considering continuum effect of soils are deemed more appropriate for studying pipe performance under tunnelling-induced settlement. These involve the two-parameter nonlinear Pasternak model (Pasternak, 1954; Liang, 2019; Lin et al., 2021) and the elastic continuum model. The Pasternak model introduces a component of shear interaction $G_{\mathrm{s}} \mathrm{d}^2 w(x)/\mathrm{d}x^2$ between soil springs, as $q(x) = k_{\mathrm{s}}^{\mathrm{t}} w(x) - G_{\mathrm{s}} \mathrm{d}^2 w(x)/\mathrm{d}x^2$, where G_{s} is the interaction parameter (Tanahashi, 2004). Its governing equation is

$$EI \frac{\mathrm{d}^4 w}{\mathrm{d}x^4} + k_{\mathrm{s}}^{\mathrm{t}} D w(x) - G_{\mathrm{s}} D \frac{\mathrm{d}^2 w}{\mathrm{d}x^2} = q(x) D, \tag{23}$$

where D is the outer diameter of the pipe. Lin et al. (2021) analyzed the deflection and bending moment of two neighbouring pipelines subject to tunnelling. The solution using Pasternak model was validated by both model tests and field observations. To account for the soil nonlinearity, Liang (2019) modified the linear Pasternak model to nonlinear, where the distributed load $q(x)$ was made equal to a hyperbolic function of settlement $w(x)$ and the shear interaction. They investigated the tunnelling heave due to unloading effect with Winkler model, linear and nonlinear Pasternak model. It was found that the deflection calculated by Pasternak model is always smaller than using Winkler model because of the consideration of interactions between adjacent soil springs. The nonlinear Pasternak model resulted in a closer match with finite element simulations and field measurements than the other models. Lin et al. (2020) waived the assumption adopted by Klar et al. (2005) that the pipe is always in contact with the soil, and explicitly considered the gap formed beneath the pipeline due to tunnelling-induced settlement. The analysis was also performed based on the Pasternak model, while the right hand side of Eq. (23) was replaced by $k_{\mathrm{s}}^{\mathrm{t}} D s(x) - G_{\mathrm{s}} D \mathrm{d}^2 s/\mathrm{d}x^2$, where $s(x)$ is the tunnelling-induced ground settlement at the depth of pipeline axis and may not necessarily equal to $w(x)$ (i.e., the profile of soil settlement at the level of pipeline axis may not be equal to the pipeline deflection when a gap exists beneath the pipe). Results from the analytical solution suggested that gap formation can reduce tunnelling-induced pipe deflection and bending moment.

The importance of proper calibration of the soil modulus $k_{\mathrm{s}}^{\mathrm{t}}$ has been highlighted by many authors (Klar et al., 2005; Liang, 2019; Ni et al., 2018b). It should be noted that the Vesic's solution was derived based on the assumption that the structure (e.g., pipe and foundation) is rested on the ground surface, while for pipes and tunnels which may be buried deep below the surface, adopting Vesic's solution of $k_{\mathrm{s}}^{\mathrm{t}}$ could give underestimated bending moments of pipes (Klar et al., 2005). Attewell et al. (1986) suggested that the modulus should be twice as the Vesic's solution for analyzing a buried pipe or tunnel. Yu et al. (2013) derived an expression of $k_{\mathrm{s}}^{\mathrm{t}}$ that is dependent on the ratio of burial depth to pipe diameter. Klar et al. (2005) also derived an alternative expression of $k_{\mathrm{s}}^{\mathrm{t}}$ that is dependent on the

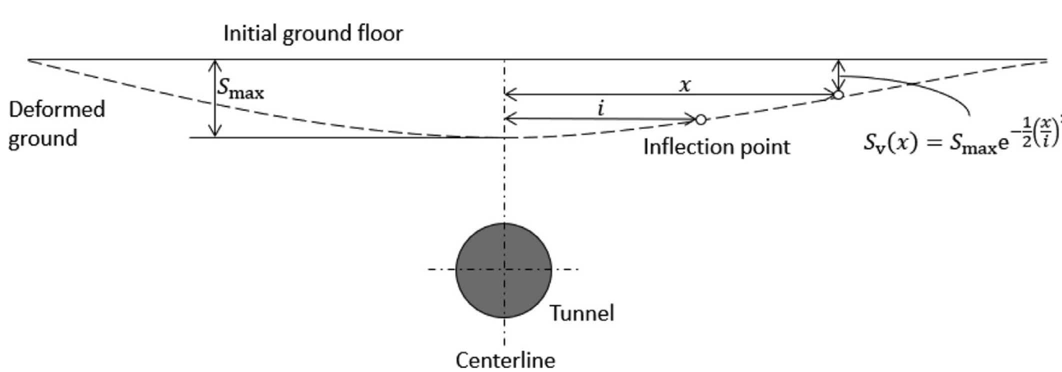

Fig. 13. Illustration for Greenfield displacement.

distance to the inflection point for analyzing pipe performance under tunnelling effect, while they found that the influence of the ratio of burial depth to pipe diameter is small.

The other method that considers the continuum effect of soil medium is the elastic continuum model, whose governing equation for a continuous pipeline can be expressed in a matrix form as Eq. (24a) (Klar et al., 2005)

$$([\boldsymbol{K}_{\mathrm{B}}] + [\boldsymbol{K}_{\mathrm{s}}] + [\boldsymbol{K}_{\mathrm{s}}][\boldsymbol{\lambda}_{\mathrm{s}}][\boldsymbol{K}_{\mathrm{B}}])\{w\} = [\boldsymbol{K}_{\mathrm{s}}]\{\boldsymbol{S}_{\mathrm{v}}\}, \tag{24a}$$

$$[\boldsymbol{K}_{\mathrm{s}}]_{i,j} = \begin{cases} \frac{1}{G_{i,j}} & i = j \\ 0 & i \neq j \end{cases}, \tag{24b}$$

$$[\boldsymbol{\lambda}_{\mathrm{s}}]_{i,j} = \begin{cases} G_{i,j} & i \neq j \\ 0 & i = j \end{cases}, \tag{24c}$$

where $[\boldsymbol{K}_{\mathrm{B}}]$ is the pipe stiffness matrix, $[\boldsymbol{K}_{\mathrm{s}}]$ is the local soil stiffness matrix and $[\boldsymbol{\lambda}_{\mathrm{s}}]$ is the alternating soil stiffness matrix. $G_{i,j}$ is the Green's function which describes soil displacement at i due to a point load at j based on the Mindlin's solution (Mindlin, 1936). The term $[\boldsymbol{K}_{\mathrm{s}}][\boldsymbol{\lambda}_{\mathrm{s}}][\boldsymbol{K}_{\mathrm{B}}]$ in Eq. (24a) represents the continuum effects, omission of which results in a solution that is similar to the Winkler model, while they are not identical because $[\boldsymbol{K}_{\mathrm{s}}]$ is different from $k_{\mathrm{s}}^{\mathrm{t}}$ using Vesic's expression. Equation (24a) can be solved either numerically (Klar et al., 2005) or using Fourier expansion method (Klar, 2018). Vorster et al. (2005) used elastic continuum method to obtain an upper bound approximation of the pipeline bending moment with an equivalent linear approach. They proposed a rigidity factor $K = EI/E_{\mathrm{s}}(D/2)i^3$ to quantify the ratio of rigidity of the pipe to the surrounding soil, and found that when $K \leq 0.1$, the pipe deflection practically follows the soil settlement profile so careful determination of the Greenfield response is necessary, while when $K \geqslant 5$ the pipe performance is dominated by pipe-soil interaction but not exact soil settlement trough. Lin et al. (2021) demonstrated the accuracy of the elastic continuum method in estimating bending performance of one pipeline and two neighbouring pipelines influenced by tunnelling. They commented that the Pasternak model can result in similar accuracy with the elastic continuum method, given that the values of $k_{\mathrm{s}}^{\mathrm{t}}$ and G_{s} are carefully calibrated.

Jointed pipelines. Klar et al. (2008) decomposed $[\boldsymbol{K}_{\mathrm{B}}]$ in Eq. (24a) to a pipe matrix $[\boldsymbol{K}_{\mathrm{p}}]$ and a joint matrix $[\boldsymbol{K}_{\mathrm{j}}]$, where the latter included a rotational stiffness $[\boldsymbol{K}_{\mathrm{jM}}]$ and a shear stiffness $[\boldsymbol{K}_{\mathrm{jS}}]$. $[\boldsymbol{K}_{\mathrm{jS}}]$ was assumed infinite so that no vertical discontinuity occurred at joints (Klar et al., 2008; Zhang et al., 2012). The solutions can be through boundary integral method (Klar et al., 2008), finite difference method (Zhang et al., 2012) or Fourier expansion with the principle of minimum potential energy (Klar, 2022). It was found that increasing the joint-to-pipe stiffness ratio increases the pipe moment but decreases the pipe displacement and joint rotation. When the joint-to-pipe stiffness ratio is zero, joints serve as hinges and the pipe suffers least bending moment while the deflection at joints are maximized.

Alternatively, beam-on-elastic-foundation method with Winkler model (Huang et al., 2019) and Pasternak model (Lin & Huang, 2019) can be used to analyze jointed pipe performance due to tunnelling. The elastic-beam governing equations (Eq. (10)) are applied to a pipe segment where the deflection is twice differentiable. Simplifications have been made for easier calculations, and the subgrade reaction on each pipe segment is uniformly distributed while the resultant force is imposed only on the center. However, the solution to rotations at both sides of a joint may rely on some numerical methods due to the discontinuity at joints.

4.2.4 Pipe uplift and upheaval buckling

Apart from downward or lateral displacement discussed above, pipes may undergo uplift displacement because of soil frost heave (Rajani & Morgenstern, 1993; Palmer & Williams, 2003; Hawlader et al., 2006; Huang et al., 2015), moisture-induced soil expansion (Singh et al., 2020) or pipe burst underneath (Chaudhuri & Choudhury, 2022). Pipe uplift displacements are different from downward or lateral displacements in that the soil resistance in the former is usually smaller than that in the latter, as noticed by Trautmann (1983). Global buckling tends to occur when pipe elevates above soil surface with low transverse resistance, while downward and lateral displacement usually do not induce global buckling since the pipe is still buried and confined in soil. Therefore, uplift soil resistance, uplift behaviour of pipes and global buckling are discussed in this part separately from the above parts.

Palmer and Williams (2003) noted that a pipe becomes unstable if uplift loads q is greater than the uplift resistance R. ASCE (1984) defined a peak uplift resistance per unit length as

$$R_{\mathrm{peak}} = \gamma' H_{\mathrm{c}} N_{\mathrm{q}} D, \tag{25}$$

where γ' is the effective weight of soil, H_{c} is the burial depth from pipe springline to the ground surface and N_{q} is a dimensionless peak uplift resistance factor. N_{q} is related to the overburden weight of soil wedge above the pipe and mobilized shear resistance of the interface between the wedge and surrounding stationary soil. Its exact formulation has not been agreed and may involve different failure mechanisms, though it is usually expressed as a function of the embedment ratio H_{c}/D and soil friction angle ϕ (Meyerhof & Adams, 1968; Murray & Geddes, 1987; Rowe & Davis, 1982; Vermeer, 1985; Vesić, 1971; White et al., 2001). Yimsiri et al. (2004) compared the above analytical N_{q} values against the experimental results by Trautmann (1983) for medium dense and dense sand, different embedment ratios and friction angles. Scatter results were observed especially when H_{c}/D and ϕ increased. Nonetheless FEM simulations with Mohr–Coulomb and Nor-Sand model fitted well with experimental results, and a design chart was made for various H_{c}/D and ϕ values. White et al. (2008) proposed a limit equilibrium solution of N_q incorporating the strength and dilatancy parameters in Bolton (1986). The solution, which did not require normality in plastic flow, estimated N_q more conservatively than the plastic solution which required the assumption of normality. Design charts were created for various values of $H_c/D, D, \phi$ and I_D. Ansari et al. (2018) proposed an alternative peak uplift resistance factor N_{vu} which was normalized against the soil shear strength at pipe springline level. N_{vu} was empirically derived with stress-dependent soil strength and dilatancy parameters from experimental uplift results. Robert and Thusyanthan (2018) performed FEM analysis on the pipe uplift resistance for unsaturated soils and it was found that existing analytical methods underpredicted N_q. An empirical equation was proposed to account for the increase of N_q contributed by matric suction.

The pipe uplift performance can also be examined analytically through the beam-on-elastic-foundation method. Hawlader et al. (2006) studied the case of soil frost heave. Uplift resistance R was segmented into elastic, post-peak degradation and residual regions, which corresponded to an increasing soil heave displacement. Parametric studies showed that post-peak reduction of R and residual resistance R_{res} significantly affect the pipe bending moment, while the rate of reduction has little influence. Singh et al. (2020) studied the case of moisture-induced soil expansion, where a vertical moist-dry interface was assumed. The method was shown to agree well with FEM results regarding pipe curvature profiles and maximum bending stress. Chaudhuri and Choudhury (2022) studied the case of a pipe bursting beneath. The ground movement was assumed to follow S_v and the soil behaviour was assumed through the Pasternak model. It was found that the critical condition in which maximum upper pipe curvature occurred was reached when the two pipelines crossed at an angle of 35°.

Upheaval buckling can be one of the failure modes for pipes buried shallow below the soil surface especially when the ratio of pipe diameter to thickness is low. Kounadis et al. (2006) derived an analytical solution to investigate the buckling behaviours of pipes through the beam-on-elastic-foundation method. Initial assumptions were made that (1) the pipe is in perfect conditions and follows a linear homogeneous differential equation; (2) the pipe is a simply supported beam; (3) the soil reaction is modeled as Winkler springs. Figure 14 shows the analytical model for analyzing pipe buckling behaviours. The governing equation is

$$EI\frac{d^4w}{dx^4} + F_a\frac{d^2w}{dx^2} + k_s^t w = 0, \tag{26}$$

where F_a denotes the axial load exerted on both sides of a pipe and L is length of pipe segment, as shown in Fig. 14. The solution to Eq. (26) is a trigonometric function and the buckled pipe shows eigen-mode shapes (Gantes & Melissianos, 2014). The critical buckling load $F_{cr} = n^2\pi^2EI/L^2 + k_s^tL^2/(n^2\pi^2)$, where $n = 1, 2, 3\cdots$ denotes the eigen-mode numbers. The initial imperfections of pipes may be considered through assuming an initial deflection of the pipe, following a sine function along the pipe axis.

4.3 Longitudinal displacement

The ground displacement parallel to the pipe longitudinal axis causes pipe wrinkling (O'Rourke et al., 1995) or tensile failure (Weerasekara & Wijewickreme, 2008, 2015), depending on the relative direction of pipe-soil displacement. To distinguish from pipe axial strain induced by the combined axial and bending strains discussed in Section 4.2.1, this part reviews analytical PSI methods solely of longitudinal pipe-soil relative displacements. Analysis of continuous and jointed pipelines is discussed in separate paragraphs.

4.3.1 Continuous pipelines

O'Rourke et al. (1995) developed analytical equations to determine steel pipe $\varepsilon_{c,max}$ for an idealized block mode longitudinal soil displacement, which was characterized by the length of soil block L_b and a constant ground displacement δ. For cases where $\varepsilon_{c,max}$ is controlled by L_b and δ, incorporating the Ramberg–Osgood stress–strain relationship, $\varepsilon_{c,max}$ was expressed as Eq. (27a) and (27b), respectively:

$$\varepsilon_{c,max} = \frac{\beta_p L_b}{2E}\left[1 + \left(\frac{n}{1+r}\right)\left(\frac{\beta_p L_b}{2\sigma_y}\right)^r\right], \tag{27a}$$

$$\varepsilon_{c,max} = \frac{\beta_p L_u}{E}\left[1 + \left(\frac{n}{1+r}\right)\left(\frac{\beta_p L_u}{\sigma_y}\right)^r\right], \tag{27b}$$

$$\frac{\delta}{2} = \int_0^{L_u} \varepsilon(x)dx, \tag{27c}$$

where n and r are Ramberg–Osgood parameters, σ_y is the yield strength, $\beta_p = \mu\gamma' H_c/t$. In Eq. (27b), L_u is the unknown length of mobilized frictional forces on pipes, which can be solved through integrating the strains within L_u, as in Eq. (27c). The analytical results accurately predicted the pipe behaviours subject to longitudinal ground displacement in the Northridge earthquake (ORourke & ORourke, 1995).

Weerasekara and Wijewickreme (2008) established analytical expressions for longitudinal PSI in which PE pipes were subject to pullout forces. The governing equations were classified as elastic, peak and post-peak ranges depending upon the mobilized pipe-soil interface friction angle δ_f. The relative pipe-soil longitudinal displacement

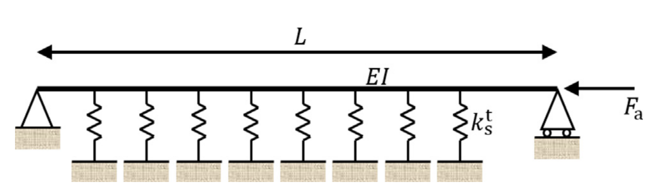

Fig. 14. Analytical model for the buckling of pipes rested on elastic foundation.

characterizing the three regions were denoted as u_e and u_p. The interface frictional resistance per unit length was

$$T = \frac{1}{2}\pi DH\gamma'(1+K)\tan\delta_f, \tag{28}$$

where K is the lateral earth pressure coefficient. The governing equations for elastic and peak ranges are shown in Eq. (29a) and Eq. (29b), respectively.

$$\frac{d}{dx}\left[EA\left(\frac{du}{dx}\right)\right] = T_p\pi D\left(\frac{u}{u_e}\right), \tag{29a}$$

$$\frac{d^2u}{dx^2} = \left(\frac{T_p}{EA}\right)\frac{\left[1+\eta\left(\frac{du}{dx}\right)\right]^3}{1-\eta\left(\frac{du}{dx}\right)}, \tag{29b}$$

where T_p is the resistance at peak and η is a model constant of the hyperbolic stress–strain relationship of PE pipes. The equation for the post-peak region was similar to Eq. (29b) except that T_p was replaced by T_{pp} denoting post-peak resistance. Axial pullout force was expressed as $F_{po} = EA(du/dx)$. Given available values for u_e, u_p and boundary conditions, the analytical relationship between pullout force and the axial strain was obtained, which matched well with experimental results. Wijewickreme and Weerasekara (2015) further improved Eq. (28) to account for the changes of normal stress on pipe caused by shear-induced soil dilation and subsequent friction degradation at large displacements. The governing equation Eq. (29) was unified without dividing the relative displacement into three regions. Instead, the pipe was segmented into small elements (e.g., x_n, x_{n+1}, etc.). The displacement, strain, force and mobilized length at each length level were computed step by step, given the boundary conditions at x_0 as $u_0 = 0$ and $du/dx = 0$.

4.3.2 Jointed pipelines

Wham and Davis (2019) proposed an analytical method to estimate axial strains developed in a jointed pipeline subject to block mode longitudinal pipe-soil relative displacement. The joints were assumed to have an axial displacement capacity Δ in both tension and compression direction, beyond which joints locked up and the pipeline behaved as a continuous one. Figure 15(a) and 15(b) illustrates the longitudinal displacements and pipe axial strains for continuous and jointed pipes, respectively. Positive strains indicate tension and negative indicate compression. For a continuous pipe, ground displacement u_g equals the sum of pipe displacement u_p; while for a jointed pipe, u_g equals the sum of u_p and a step-wised joint displacement u_j, with a constant step height Δ. γ_p in Fig. 15(b) denotes the strain capacity of joints of a pipe segment defined by the ratio of Δ to the length of a pipe segment h, and l_s is the length of a pipe with relative pipe-soil displacement. With the addition of joints, and assuming joints lock up consecutively, the governing equation for axial strain is $\varepsilon_a = (Tl_s)/(EA)$. Solving for l_s, ε_a can be expressed as

$$\varepsilon_a = -\gamma_p \pm \sqrt{\gamma_p^2 + \frac{Td_T}{EA}}, \tag{30}$$

where d_T is the total displacement due to pipe elongation and joint lock-up. Wham and Davis (2019) expressed the maximum axial strain $\varepsilon_{a,max}$ in two different scenarios, depending upon whether L_b exceeded $2l_s$. And Fig. 15 presents the case for $L_b > 2l_s$ as an example. This analytical method was validated against numerical simulations in Banushi and Wham (2021) where an excellent match was observed. Larger Δ improved the capacity for a pipe to accommodate longitudinal pipe-soil relative displacement.

5 Future research opportunities

The study of PSI analytical methods involves multiple problems of interest and research methods. Therefore opportunities for future research are broad. This part discusses some possible research paths that might be of interest to researchers.

5.1 The role of friction in cross-sectional deformation

The pipe cross-sectional deformation consists of ovalization or circumferential shortening. The deformation formulations considered the effects of pipe and backfill stiffness individually, but did not account for the influence of friction at the interface between the pipe walls and the surrounding soils on the cross-sectional deformation. It is well known that soil-structure interface problems are a function of friction, like skin friction or shaft resistance of piles. Though omitting the friction should be more conservative from the perspective of engineering design, it is physically rational to consider pipe-soil interface friction, which is the same as in the analysis of relative pipe-soil displacement in transverse and longitudinal directions.

5.2 Combined effects of bending and compression

Analytical methods adopting the beam-on-elastic-foundation method usually investigated the bending and tensile failure of pipes buried in soil. Their accuracy in estimating the performance of a pipe crossing a fault with a small angle has been demonstrated, while a large discrepancy from numerical results exists when the fault-crossing angle is large. This implies that the analytical solutions have not correctly accounted for the combined effects of bending and compression. The assumption that the pipe is always in contact with the soil, which has been adopted in many analysis, may not be true in cases of large pipe deflections.

5.3 Choice of soil reaction models and calibration of key parameters

The efficacy of analytical solutions to PSI problems is largely dependent on the choice of soil reaction models

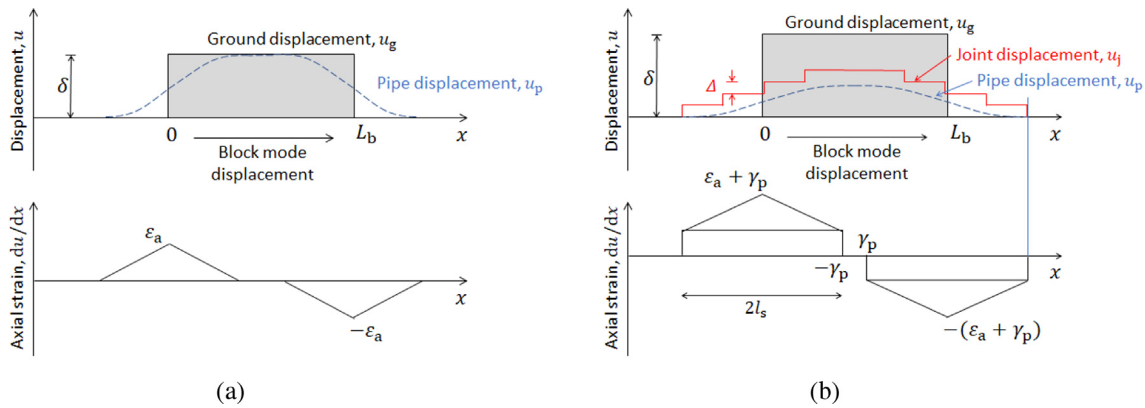

Fig. 15. Illustration for longitudinal pipe-soil relative displacement and pipe axial strain. (a) Continuous pipe, and (b) jointed pipe.

(e.g., Winkler model, Pasternak model and elastic continuum model) and proper values of key parameters in the models, such as the soil modulus E' for calculating cross-sectional deformation, subgrade modulus k_s^t in the beam method and the uplift resistance factor N_q in evaluating the pipe uplift. The feasibility of applying a soil reaction model to analyzing pipe performance under different pipe and soil conditions should be further clarified. There is some disagreement in selecting values of the key parameters (e.g., k_s^t and N_q) which may result in inaccurate and unsafe estimations of pipe performance. Proper calibration of these key parameters is beneficial for a more appropriate representation of pipe performance and soil reactions.

5.4 Effect of pipe flaws

Existing analytical methods usually assumed that the pipe being studied is intact and robust. While in real circumstances pipe may be more vulnerable to breakage or failure at flawed positions, such as corrosion and oxidation pits. These positions may be associated with a decrease in pipe thickness, stiffness or strength. The inclusion of pipe flaws in the analytical methods could be more realistic and persuasive. A possible approach could be treating these flawed positions as joints with reduced strengths, stiffness or deformation capacities.

5.5 Soil spatial variability

Existing analytical methods usually assumed that the surrounding soil is homogeneous. Only a few studies took into account the effect of soil stratification, where the pipe longitudinal axis was parallel to the plane of strata. Soil spatial variability is not limited to horizontal stratification and can have negative effects on pipe performance. For example, pipes may cross inclined strata, be supported by soil foundations with varying stiffness or be adjacent to local stiffened zones (e.g., granite in soil layers; this is relative to the case of weak soil zones). Possible methods could be segmenting the pipes into different regions according to spatial variability of soil properties, with compatibility of deformation and appropriate boundary conditions.

5.6 Behaviours of curved pipes

It seems that most analytical methods have been applied to straight pipes. Curved portions of a buried pipe are also vulnerable to breakage due to internal and external loads. Thrust restraint design relies on a proper understanding of PSI and may be analyzed through beam method as well. However, research in this area is largely absent and needs more attention.

6 Conclusions

Buried pipelines are vulnerable to failure or breakage due to excessive loads or ground displacements. A proper understanding of pipe-soil interaction (PSI) is the key to an accurate evaluation of pipe performance and serviceability. Analytical methods hold the merits of fast calculation, low requirement of computational resources and acceptable accuracy. They also provide a physical rationale to understand how pipes interact with surrounding soils. A comprehensive review in such a topic can benefit researchers that are new to this area to quickly get familiar with relevant works and find possible research paths. This study conducted a systematic and thorough literature review on studying PSI problems using analytical methods. Both scientometric analysis and qualitative analysis were presented, based on which possible future research paths were given. The main conclusions are as follows:

- The results from scientometric analysis found some representative journals in which many published articles were collected in this review. The names of authors that frequently showed up with their focuses of study were also presented. Network analysis of the article keywords identified some of the scenarios that have been investigated and models that have been adopted in studying PSI problems analytically. These serve as a guidance to researchers that are new to this area and help them quickly access the relevant works.

- Qualitative analysis was performed through technically reviewing the progress in analytical methods for studying PSI problems in cross-sectional, transverse and longitudinal directions. In cross-sectional analysis, areas of study were concentrated on the ovalization deformation and such works have been improved based on the Iowa formula. In analysis where load and deformation are transverse to the pipeline axis, the scenarios were classified into seismic faults, weak soil zones, ground settlement and pipe uplift. In these analysis the most common method should be the beam on elastic method that assumes the pipeline as an elastic beam rested on elastic soil foundations. Multiple soil models were reviewed with their strengths and weaknesses discussed. The governing equations of each model were elaborated and solution methods were introduced. The importance of key parameters in the soil models was identified. The different behaviours of continuous and segmented pipelines were introduced, with the applicability of the soil models. In the analysis of pipe performance subject to longitudinal pipe-soil relative displacement, the governing equations were introduced. Analysis on both continuous and segmented pipes was performed.
- Six possible paths for future research works were found, which are (1) the role of friction in cross-sectional deformation, (2) combined effects of bending and compression, (3) choice of soil reaction models and calibration of key parameters, (4) effect of pipe flaws, (5) soil spatial variability and (6) behaviours of curved pipes.

Declaration of Competing Interest

The authors declare that they have no known competing financial interests or personal relationships that could have appeared to influence the work reported in this paper.

Acknowledgement

The authors gratefully acknowledge the Innovation and Technology Support Programme (ITSP) [Grant No. ITS/033/20FP] and the Water Supplies Department of Hong Kong, China. Suggestions given by Dr. Andy Y. F. Leung are also appreciated.

References

Akagawa, S., Huang, S.L., Kanie, S., & Fukuda, M. (2012). Movement due to heave and thaw settlement of a full-scale test chilled gas pipeline constructed in fairbanks alaska. *Otc arctic technology conference, December 3*. Houston, Texas, USA.

ALA (2001). *Guidelines for the design of buried steel pipe*. American Lifelines Alliance.

Ansari, Y., Kouretzis, G., & Sloan, S. W. (2018). Development of a prototype for modelling soil–pipe interaction and its application for predicting uplift resistance to buried pipe movements in sand. *Canadian Geotechnical Journal, 55*(10), 1451–1474.

ASCE (1984). *Guidelines for the seismic design of oil and gas pipeline systems*. American Society of Civil Engineers.

Attewell, P. B., Yeates, J., & Selby, A. R. (1986). *Soil movements induced by tunnelling and their effects on pipelines and structures*. New York, NY: Methuen, Inc..

Banushi, G., & Wham, B. P. (2021). Deformation capacity of buried hybrid-segmented pipelines under longitudinal permanent ground deformation. *Canadian Geotechnical Journal, 58*(8), 1095–1117.

Barton, N. A., Farewell, T. S., Hallett, S. H., & Acland, T. F. (2019). Improving pipe failure predictions: Factors effecting pipe failure in drinking water networks. *Water Research, 164*, 114926.

Bolton, M. D. (1986). The strength and dilatancy of sands. *Géotechnique, 36*, 65–78.

Bowles, L. M., Duke, W. C., & Brown, T. P. (2019). *Method for prediction of flexible pipe deflection*. Denver: Technical Service Center.

Brachman, R., Moore, I., & Munro, S. (2008). Compaction effects on strains within profiled thermoplastic pipes. *Geosynthetics International, 15*(2), 72–85.

Britannica, The Editors of Encyclopedia. (2022). Strike-slip fault. Encyclopedia Britannica. https://www.britannica.com/science/strike-slip-fault.

Calvetti, F., Di Prisco, C., & Nova, R. (2004). Experimental and numerical analysis of soil–pipe interaction. *Journal of Geotechnical and Geoenvironmental Engineering, 130*(12), 1292–1299.

Chaudhuri, C. H., & Choudhury, D. (2020). Buried pipeline subjected to seismic landslide: A simplified analytical solution. *Soil Dynamics and Earthquake Engineering, 134*, 106155.

Chaudhuri, C. H., & Choudhury, D. (2022). Buried pipeline subjected to static pipe bursting underneath: A closed-form analytical solution. *Géotechnique, 72*(11), 974–983.

Cocchetti, G., di Prisco, C., Galli, A., & Nova, R. (2009). Soil–pipeline interaction along unstable slopes: A coupled three-dimensional approach. part 1: Theoretical formulation. *Canadian Geotechnical Journal, 46*(11), 1289–1304.

Cubrinovski, M., Bradley, B., Wotherspoon, L., Green, R., Bray, J., Wood, C., Pender, M., Allen, J., Bradshaw, A., Rix, G., et al. (2011). Geotechnical aspects of the 22 february 2011 christchurch earthquake. *Bulletin of the New Zealand Society for Earthquake Engineering, 44*(4), 205–226.

Gantes, C. J., & Melissianos, V. E. (2014). Buckling and post-buckling behavior of beams on elastic foundation modeling buried pipelines. In *Cesare'14. civil engineering for sustainability and resilience international conference*.

Ghavami, P. (2014). *Mechanics of materials: An introduction to engineering technology*. Springer.

Hartley, J. D., & Duncan, J. M. (1987). E' and its variation with depth. *Journal of Transportation Engineering, 113*(5), 538–553.

Hawlader, B. C., Morgan, V., & Clark, J. I. (2006). Modelling of pipeline under differential frost heave considering post-peak reduction of uplift resistance in frozen soil. *Canadian Geotechnical Journal, 43*(3), 282–293.

Hetényi, M., & Hetbenyi, M. I. (1946). *Beams on elastic foundation: Theory with applications in the fields of civil and mechanical engineering* (Vol. 16). MI: University of Michigan press Ann Arbor.

Hou, Y., Fang, Q., Zhang, D., & Wong, L. N. Y. (2015). Excavation failure due to pipeline damage during shallow tunnelling in soft ground. *Tunnelling and Underground Space Technology, 46*, 76–84.

Howard, A. K. (1977). Modulus of soil reaction values for buried flexible pipe. *Journal of the Geotechnical Engineering Division, 103*(1), 33–43.

Hsu, T. W., Chen, Y. J., & Hung, W. C. (2006). Soil friction restraint of oblique pipelines in dense sand. *Journal of Transportation Engineering, 132*(2), 175–181.

Hsu, T. W., Chen, Y. J., & Wu, C. Y. (2001). Soil friction restraint of oblique pipelines in loose sand. *Journal of Transportation Engineering, 127*(1), 82–87.

Hu, W., Zhao, Y., Hu, K., Chen, G., & Fu, K. (2022). A new analytical method for calculating the strain of oil and gas pipeline under a normal fault dislocation. In *Energy Science and Engineering*.

Hu, Z., Ren, X., Wang, Q., Wang, R., & Pan, R. (2022). Analytical method for the mechanical response of buried pipeline under the action of strike-slip faulting. *Underground Space, 7*(2), 268–277.

Huang, M., Zhou, X., Yu, J., Leung, C., & Tan, J. Q. W. (2019). Estimating the effects of tunnelling on existing jointed pipelines based on winkler model. *Tunnelling and Underground Space Technology, 86*, 89–99.

Huang, S. L., Yang, K., Akagawa, S., Fukuda, M., & Kanie, S. (2015). Frost heave induced pipe strain of an experimental chilled gas pipeline. In *Innovative materials and design for sustainable transportation infrastructure* (pp. 405–416). American Society of Civil Engineers.

Ieronymaki, E. S., & Whittle, A. J. (2017). Pipeline response to ground deformations induced by tunneling. In *Geotechnical frontiers, March 12-15, 2017, Orlando, Florida* (pp. 566–575). American Society of Civil Engineers.

Iimura, S. (2004). Simplified mechanical model for evaluating stress in pipeline subject to settlement. *Construction and Building Materials, 18*(6), 469–479.

Imanzadeh, S., Denis, A., & Marache, A. (2013). Simplified uncertainties analysis of continuous buried steel pipes on an elastic foundation in the presence of low stiffness zones. *Computers and Geotechnics, 48*, 62–71.

Imanzadeh, S., Marache, A., & Denis, A. (2017). Influence of soil spatial variability on possible dysfunction and failure of buried pipe, case study in Pessac city, France. *Environmental Earth Sciences, 76*(5), 212.

Jeyapalan, J. K., & Watkins, R. (2004). Modulus of soil reaction (e') values for pipeline design. *Journal of Transportation Engineering, 130*(1), 43–48.

Karamitros, D. K., Bouckovalas, G. D., & Kouretzis, G. P. (2007). Stress analysis of buried steel pipelines at strike-slip fault crossings. *Soil Dynamics and Earthquake Engineering, 27*(3), 200–211.

Karamitros, D. K., Bouckovalas, G. D., Kouretzis, G. P., & Gkesouli, V. (2011). An analytical method for strength verification of buried steel pipelines at normal fault crossings. *Soil Dynamics and Earthquake Engineering, 31*(11), 1452–1464.

Kennedy, R. P., Williamson, R. A., & Chow, A. M. (1977). Fault movement effects on buried oil pipeline. *Transportation Engineering Journal of ASCE, 103*(5), 617–633.

Klar, A. (2018). Elastic continuum solution for tunneling effects on buried pipelines using fourier expansion. *Journal of Geotechnical and Geoenvironmental Engineering, 144*(9), 04018062.

Klar, A. (2022). A fourier-based elastic continuum solution for jointed pipeline response to tunneling. *Tunnelling and Underground Space Technology, 119*, 104237.

Klar, A., Marshall, A. M., Soga, K., & Mair, R. J. (2008). Tunneling effects on jointed pipelines. *Canadian Geotechnical Journal, 45*(1), 131–139.

Klar, A., Vorster, T., Soga, K., & Mair, R. (2005). Soil—pipe interaction due to tunnelling: Comparison between winkler and elastic continuum solutions. *Géotechnique, 55*(6), 461–466.

Kounadis, A., Mallis, J., & Sbarounis, A. (2006). Postbuckling analysis of columns resting on an elastic foundation. *Archive of Applied Mechanics, 75*(6), 395–404.

Kouretzis, G. P., Karamitros, D., & Sloan, S. W. (2015). Analysis of buried pipelines subjected to ground surface settlement and heave. *Canadian Geotechnical Journal, 52*, 1058–1071.

Leonhard, G. (1973). *Die belastungen von starren rohrleitungen unter dämmen, diss* Unpublished doctoral dissertation. TU Hannover.

Li, H., Lai, Y., Wang, L., Yang, X., Jiang, N., Li, L., Wang, C., & Yang, B. (2019). Review of the state of the art: Interactions between a buried pipeline and frozen soil. *Cold Regions Science and Technology, 157*, 171–186.

Li, Y., Jin, H., Wen, Z., Li, X., & Zhang, Q. (2021). Stability of the foundation of buried energy pipeline in permafrost region. *Geofluids, 2021*, 3066553.

Liang, R. (2019). Simplified analytical method for evaluating the effects of overcrossing tunnelling on existing shield tunnels using the nonlinear pasternak foundation model. *Soils and Foundations, 59*(6), 1711–1727.

Lin, C., & Huang, M. (2019). Tunnelling-induced response of a jointed pipeline and its equivalence to a continuous structure. *Soils and Foundations, 59*(4), 828–839.

Lin, C., Huang, M., Nadim, F., & Liu, Z. (2020). Tunnelling-induced response of buried pipelines and their effects on ground settlements. *Tunnelling and Underground Space Technology, 96*, 103193.

Lin, C., Huang, M., Nadim, F., Liu, Z., & Yu, J. (2021). Analytical solutions for tunnelling-induced response of two overlying pipelines. *Tunnelling and Underground Space Technology, 108*, 103678.

Liu, A., Hu, Y., Zhao, F., Li, X., Takada, S., & Zhao, L. (2004). An equivalent-boundary method for the shell analysis of buried pipelines under fault movement. *Acta Seismologica Sinica, 17*(1), 150–156.

Liu, M., & Ortega, R. (2021). Thrust restraint of buried continuous pressure pipe considering pipe–soil interaction. *Journal of Pipeline Systems Engineering and Practice, 12*(4), 04021039.

Macaro, G., Utili, S., & Martin, C. M. (2021). Dem simulations of transverse pipe–soil interaction on sand. *Géotechnique, 71*(3), 189–204.

Makar, J., Desnoyers, R., & McDonald, S. (2020). Failure modes and mechanisms in gray cast iron pipes. In *Underground infrastructure research* (pp. 303–312). CRC Press.

Marshall, A., Elkayam, I., Klar, A., & Mair, R. (2010). Centrifuge and discrete element modelling of tunnelling effects on pipelines. In *Proceedings of the 7th international conference on physical modelling in geotechnics* (pp. 633–637).

Marston, A. (1930). The theory of external loads on closed conduits in the light of the latest experiments. In *Highway research board proceedings* (Vol. 9).

Masada, T. (1996). *Structural performance of profile-wall plastic pipes under relatively shallow soil cover and subjected to large surface load.* Ohio University.

Masada, T. (2000). Modified iowa formula for vertical deflection of buried flexible pipe. *Journal of Transportation Engineering, 126*(5), 440–446.

Masada, T., & Sargand, S. M. (2007). Peaking deflections of flexible pipe during initial backfilling process. *Journal of Transportation Engineering, 133*(2), 105–111.

Melissianos, V. E., & Gantes, C. J. (2016). Buckling and post-buckling behavior of beams with internal flexible joints resting on elastic foundation modeling buried pipelines. *Structures, 7*, 138–152.

Meyerhof, G., & Adams, J. (1968). The ultimate uplift capacity of foundations. *Canadian Geotechnical Journal, 5*(4), 225–244.

Mindlin, R. D. (1936). Force at a point in the interior of a semi-infinite solid. *Physics, 7*(5), 195–202.

Moore, I. D. (2001). Buried pipes and culverts. In *Geotechnical and geoenvironmental engineering handbook* (pp. 541–567). Springer.

Moser, A. (1994). *The structural performance of buried 48 inch diameter n-12 hc polyethylene pipes*. Logan, Utah: Buried Structural Laboratory, Utah State University.

Moser, A., & Folkman, S. (2008). *Buried pipe design*. McGraw-Hill Education.

Murray, E., & Geddes, J. D. (1987). Uplift of anchor plates in sand. *Journal of Geotechnical Engineering, 113*(3), 202–215.

Newmark, N. M., & Hall, W. J. (1975). Pipeline design to resist large fault displacement. *Proceedings of us national conference on earthquake engineering, June 18–20, Ann Arbor, Michigan, US, Vol. 1975*, 416–425.

Ni, P., & Mangalathu, S. (2018a). Fragility analysis of gray iron pipelines subjected to tunneling induced ground settlement. *Tunnelling and Underground Space Technology, 76*, 133–144.

Ni, P., & Mangalathu, S. (2018b). Simplified evaluation of pipe strains crossing a normal fault through the dissipated energy method. *Engineering Structures, 167*, 393–406.

Ni, P., Mangalathu, S., & Liu, K. (2020). Enhanced fragility analysis of buried pipelines through lasso regression. *Acta Geotechnica, 15*(2), 471–487.

Ni, P., Mangalathu, S., & Yi, Y. (2018). Fragility analysis of continuous pipelines subjected to transverse permanent ground deformation. *Soils and Foundations, 58*(6), 1400–1413.

Ni, P., Moore, I., & Take, W. (2018a). Distributed fibre optic sensing of strains on buried full-scale pvc pipelines crossing a normal fault. *Géotechnique, 68*(1), 1–17.

Nixon, J., & Oswell, J. M. (2010). Analytical solutions for peak and residual uplift resistance of pipelines. In *Proceedings 63rd canadian geotechnical conference and 6th canadian permafrost conference, September 12–15, Calgary, Alberta* (pp. 570–578).

Ni, P., Moore, I. D., & Take, W. A. (2018b). Numerical modeling of normal fault-pipeline interaction and comparison with centrifuge tests. *Soil Dynamics and Earthquake Engineering, 105*, 127–138.

O'Rourke, M. J., & Liu, X. (1999). *Response of buried pipelines subject to earthquake effects.* Mceer New York.

O'Rourke, M. J., Liu, X., & Flores-Berrones, R. (1995). Steel pipe wrinkling due to longitudinal permanent ground deformation. *Journal of Transportation Engineering, 121*(5), 443–451.

ORourke, T., & ORourke, M. (1995). *Pipeline response to permanent ground deformation: A benchmark case (Tech. Rep.)*. New York, NY (United States): American Society of Civil Engineers.

O'Rourke, M. J., & Liu, X. (2012). Seismic design of buried and offshore pipelines. MCEER Monograph MCEER-12-MN04, 380.

Palmer, A. C., & Williams, P. J. (2003). Frost heave and pipeline upheaval buckling. *Canadian Geotechnical Journal, 40*(5), 1033–1038.

Paolucci, R., Griffini, S., & Mariani, S. (2010). Simplified modelling of continous buried pipelines subject to earthquake fault rupture. *Earthquakes and Structures, 1*(3), 253–267.
Pasternak, P. (1954). *On a new method of an elastic foundation by means of two foundation constants*. Moscow, Russia: Gosudarstvennoe Izdatelstvo Literaturi po Stroitelstuve i Arkhitekture.
Qin, X., & Ni, P. (2019). Kinematics of bell-spigot joints in vitrified clay pipelines under differential ground movement. *Tunnelling and Underground Space Technology, 91*, 103005.
Qin, X., Ni, P., & Du, Y. (2019). Buried rigid pipe-soil interaction in dense and medium sand backfills under downward relative movement: 2d finite element analysis. *Transportation Geotechnics, 21*, 100286.
Qin, X., Ni, P., Wang, Y., & Du, Y. (2021). Mechanical response estimation of jointed rigid pipes under normal fault rupture. *Soil Dynamics and Earthquake Engineering, 146*, 106754.
Qin, X., & Wang, Y. (2022). Different failure modes assessment of bell-spigot jointed ductile iron pipes under abrupt transverse ground movements. *Soil Dynamics and Earthquake Engineering, 163*, 107558.
Qin, X., Wang, Y., & Fu, C. (2022). Joint kinematics and sealing capacity assessment of ductile iron pipes under abrupt transverse ground movements. *Canadian Geotechnical Journal, 59*(3), 342–358.
Rajani, B., & Abdel-Akher, A. (2013). Performance of cast-iron-pipe bell-spigot joints subjected to overburden pressure and ground movement. *Journal of Pipeline Systems Engineering and Practice, 4*(2), 98–114.
Rajani, B., & Morgenstern, N. (1993). Pipelines and laterally loaded piles in elastoplastic medium. *Journal of Geotechnical Engineering, 119*(9), 1431–1448.
Rajani, B., & Tesfamariam, S. (2004). Uncoupled axial, flexural, and circumferential pipe soil interaction analyses of partially supported jointed water mains. *Canadian Geotechnical Journal, 41*(6), 997–1010.
Rajani, B., Zhan, C., & Kuraoka, S. (1996). Pipe soil interaction analysis of jointed water mains. *Canadian Geotechnical Journal, 33*(3), 393–404.
Rajeev, P., Kodikara, J., Robert, D., Zeman, P., & Rajani, B. (2014). Factors contributing to large diameter water pipe failure. *Water Asset Management International, 10*(3), 9–14.
Ramberg, W., & Osgood, W. R. (1943). *Description of stress-strain curves by three parameters*. Washington, USA: NASA Scientific and Technical Information Facility.
Richard B., W. (2000). *Atv-dvwk-a 127e: Static calculation of drains and sewers*. DWA German Association for Water, Wastewater and Waste.
Robert, D., & Thusyanthan, N. (2018). Uplift resistance of buried pipelines in partially saturated sands. *Computers and Geotechnics, 97*, 7–19.
Rowe, R., & Davis, E. (1982). The behaviour of anchor plates in sand. *Géotechnique, 32*(1), 25–41.
Saberi, M., Behnamfar, F., & Vafaeian, M. (2013). A semi-analytical model for estimating seismic behavior of buried steel pipes at bend point under propagating waves. *Bulletin of Earthquake Engineering, 11*(5), 1373–1402.
Saiyar, M., Ni, P., Take, W., & Moore, I. (2016). Response of pipelines of differing flexural stiffness to normal faulting. *Géotechnique, 66*(4), 275–286.
Sargand, S. (2002). Field verification of structural performance of thermoplastic pipe under deep backfill conditions. *NASA STI/Recon Technical Report N, 3*, 14339.
Sargand, S., Masada, T., Tarawneh, B., & Gruver, D. (2005). Field performance and analysis of large-diameter high-density polyethylene pipe under deep soil fill. *Journal of Geotechnical and Geoenvironmental Engineering, 131*(1), 39–51.
Sargand, S. M., & Masada, T. (2003). Soil arching over deeply buried thermoplastic pipe. *Transportation research record, 1849*(1), 109–123.
Sarvanis, G. C., & Karamanos, S. A. (2017). Analytical model for the strain analysis of continuous buried pipelines in geohazard areas. *Engineering structures, 152*, 57–69.
Shao, Y., & Zhang, T.-Q. (2008). Elastoplastic pipe-soil interaction analyses of partially-supported jointed water mains. *Journal of Zhejiang University-SCIENCE A, 9*(11), 1497–1506.
Sheil, B. B., Martin, C. M., & Byrne, B. W. (2021). Simulation of overburden pressure during laboratory investigations of axial pipe–soil interaction. *Géotechnique, 71*(3), 272–278.
Singh, P. R., Pericoli, V., Kanvinde, A., & Narasimhan, S. (2020). Framework for analyzing cast iron water main fractures due to moisture-induced soil expansion. *Journal of Pipeline Systems Engineering and Practice, 11*(3), 04020015.
Sivakumar Babu, G., Srinivasa Murthy, B., & Seshagiri Rao, R. (2006). Reliability analysis of deflection of buried flexible pipes. *Journal of Transportation Engineering, 132*(10), 829–836.
Spangler, M. G., & Shafer, G. (1938). The structural design of flexible pipe culverts. In *Highway research board proceedings* (Vol. 17, p. 235–239).
Takada, S., Hassani, N., & Fukuda, K. (2001). A new proposal for simplified design of buried steel pipes crossing active faults. *Earthquake Engineering & Structural Dynamics, 30*(8), 1243–1257.
Talebi, F., & Kiyono, J. (2020). Introduction of the axial force terms to governing equation for buried pipeline subjected to strike-slip fault movements. *Soil Dynamics and Earthquake Engineering, 133*, 106125.
Talebi, F., & Kiyono, J. (2021). A refined nonlinear analytical method for buried pipelines crossing strike-slip faults. *Earthquake Engineering & Structural Dynamics, 50*(11), 2915–2938.
Tanahashi, H. (2004). Formulas for an infinitely long bernoulli-euler beam on the pasternak model. *Soils and Foundations, 44*(5), 109–118.
Tariq, S., Hu, Z., & Zayed, T. (2021). Micro-electromechanical systems-based technologies for leak detection and localization in water supply networks: A bibliometric and systematic review. *Journal of Cleaner Production, 289*, 125751.
Tawfik, G. M., Dila, K. A. S., Mohamed, M. Y. F., Tam, D. N. H., Kien, N. D., Ahmed, A. M., & Huy, N. T. (2019). A step by step guide for conducting a systematic review and meta-analysis with simulation data. *Tropical Medicine and Health, 47*(1), 1–9.
Tesfamariam, S., Rajani, B., & Sadiq, R. (2006). Possibilistic approach for consideration of uncertainties to estimate structural capacity of ageing cast iron water mains. *Canadian Journal of Civil Engineering, 33*(8), 1050–1064.
Timoshenko, S., & Goodier, J. N. (1951). *Theory of elasticity*. McGraw-Hill.
Tokimatsu, K., Tamura, S., Suzuki, H., & Katsumata, K. (2012). Building damage associated with geotechnical problems in the 2011 tohoku pacific earthquake. *Soils and Foundations, 52*(5), 956–974.
Trautmann, C. H. (1983). *Behavior of pipe in dry sand under lateral and uplift loading* Unpublished doctoral dissertation. Cornell University.
Trifonov, O. V. (2018). The effect of variation of soil conditions along the pipeline in the fault-crossing zone. *Soil Dynamics and Earthquake Engineering, 104*, 437–448.
Trifonov, O. V., & Cherniy, V. P. (2010). A semi-analytical approach to a nonlinear stress–strain analysis of buried steel pipelines crossing active faults. *Soil Dynamics and Earthquake Engineering, 30*(11), 1298–1308.
Trifonov, O. V., & Cherniy, V. P. (2012). Elastoplastic stress–strain analysis of buried steel pipelines subjected to fault displacements with account for service loads. *Soil Dynamics and Earthquake Engineering, 33*(1), 54–62.
Trifonov, V., Oleg, Cherniy, P., & Vladimir. (2011). Analytical model versus numerical model in stress-strain analysis of buried steel pipelines subjected to fault displacements. In *Iii eccomas thematic conference on computational methods in structural dynamics and earthquake engineering, May 25–28, Corfu, Greece*. Citeseer.
Tsinidis, G., Di Sarno, L., Sextos, A., & Furtner, P. (2019). A critical review on the vulnerability assessment of natural gas pipelines subjected to seismic wave propagation. part 2: Pipe analysis aspects. *Tunnelling and Underground Space Technology, 92*, 103056.
Valsamis, A. I., & Bouckovalas, G. D. (2020). Analytical methodology for the verification of buried steel pipelines with flexible joints crossing strike-slip faults. *Soil Dynamics and Earthquake Engineering, 138*, 106280.
van Eck, N. J., & Waltman, L. (2010). Vosviewer: Visualizing scientific landscapes [software version 1.6.17]. https://www.vosviewer.com.
Vazouras, P., Dakoulas, P., & Karamanos, S. A. (2015). Pipe–soil interaction and pipeline performance under strike–slip fault movements. *Soil Dynamics and Earthquake Engineering, 72*, 48–65.
Vazouras, P., Karamanos, S. A., & Dakoulas, P. (2010). Finite element analysis of buried steel pipelines under strike-slip fault displacements. *Soil Dynamics and Earthquake Engineering, 30*(11), 1361–1376.
Vazouras, P., Karamanos, S. A., & Dakoulas, P. (2012). Mechanical behavior of buried steel pipes crossing active strike-slip faults. *Soil Dynamics and Earthquake Engineering, 41*, 164–180.
Vermeer, P. (1985). The uplift resistance of shallow embedded anchors. In *Proc. 11th. int. conf. on smfe, aug. 12, San Francisco, CA, USA* (pp. 1635–1938).
Vesić, A. B. (1961). Bending of beams resting on isotropic elastic solid. *Journal of the Engineering Mechanics Division, 87*(2), 35–53.

Vesić, A. S. (1971). Breakout resistance of objects embedded in ocean bottom. *Journal of the Soil Mechanics and Foundations Division, 97*(9), 1183–1205.

Vorster, T., Klar, A., Soga, K., & Mair, R. (2005). Estimating the effects of tunneling on existing pipelines. *Journal of Geotechnical and Geoenvironmental Engineering, 131*(11), 1399–1410.

Wang, B., Li, X., & Zhou, J. (2011). Strain analysis of buried steel pipelines across strike-slip faults. *Journal of Central South University of Technology, 18*(5), 1654.

Wang, L. R., & Yeh, Y. (1985). A refined seismic analysis and design of buried pipeline for fault movement. *Earthquake Engineering & Structural Dynamics, 13*(1), 75–96.

Wang, Y., & Moore, I. D. (2014). Simplified design equations for joints in buried flexible pipes based on hetényi solutions. *Journal of Geotechnical and Geoenvironmental Engineering, 140*(3), 04013020.

Wang, Y., & Moore, I. D. (2015). Simplified design model for rigid pipe joints based on the two-pipe approximation. *Canadian Geotechnical Journal, 52*(5), 626–637.

Wang, Y., Wang, Q., & Zhang, K. (2011). An analytical model for pipe-soil-tunneling interaction. *Procedia Engineering, 14*, 3127–3135.

Wang, Y. H., Tham, L. G., & Cheung, Y. K. (2005). Beams and plates on elastic foundations: A review. *Progress in Structural Engineering and Materials, 7*(4), 174–182.

Watkins, R. K., & Spangler, M. (1958). Some characteristics of the modulus of passive resistance of soil: A study in similitude. In *Highway research board proceedings* (Vol. 37, p. 576–583).

Weerasekara, L., & Wijewickreme, D. (2008). Mobilization of soil loads on buried, polyethylene natural gas pipelines subject to relative axial displacements. *Canadian Geotechnical Journal, 45*(9), 1237–1249.

Wham, B. P., & Davis, C. A. (2019). Buried continuous and segmented pipelines subjected to longitudinal permanent ground deformation. *Journal of Pipeline Systems Engineering and Practice, 10*(4), 04019036.

White, D., Barefoot, A., & Bolton, M. (2001). Centrifuge modelling of upheaval buckling in sand. *International Journal of Physical Modelling in Geotechnics, 1*(2), 19–28.

White, D., Cheuk, C., & Bolton, M. (2008). The uplift resistance of pipes and plate anchors buried in sand. *Géotechnique, 58*(10), 771–779.

Wijewickreme, D., & Weerasekara, L. (2015). Analytical modeling of field axial pullout tests performed on buried extensible pipes. *International Journal of Geomechanics, 15*(2), 04014044.

WSD. (2022). Water Supplies Department, The Government of Hong Kong Special Administrative Region. http://www.wsd.gov.hk/en/home/index.html. (Access date: 16.09.2022)

Xia, M., & Zhang, H. (2017). An analytical approach for strain analysis of buried steel pipeline in mining subsidence areas. In *Pressure vessels and piping conference* (Vol. 57984, p. V005T11A010).

Xu, G., Qi, J., & Jin, H. (2010). Model test study on influence of freezing and thawing on the crude oil pipeline in cold regions. *Cold Regions Science and Technology, 64*(3), 262–270.

Xu, R., Jiang, R., & Qu, T.-J. (2021). Review of dynamic response of buried pipelines. *Journal of Pipeline Systems Engineering and Practice, 12*(2), 03120003.

Xu, X., He, K., & Su, Y. (2020). Safety analysis of pipe–soil coordination deformation affected by mining subsidence. *Geotechnical and Geological Engineering, 38*(2), 2187–2198.

Yimsiri, S., Soga, K., Yoshizaki, K., Dasari, G., & O'Rourke, T. (2004). Lateral and upward soil-pipeline interactions in sand for deep embedment conditions. *Journal of Geotechnical and Geoenvironmental Engineering, 130*(8), 830–842.

Yoo, C. S., Choi, B., & Jung, H. (2005). Excavation-induced buried pipeline failure – A case study. *Solid State Phenomena, 110*, 23–30.

Yu, J., Zhang, C., & Huang, M. (2013). Soil–pipe interaction due to tunnelling: Assessment of winkler modulus for underground pipelines. *Computers and Geotechnics, 50*, 17–28.

Zhai, K., Wang, F., Fang, H., Ni, P., Ji, X., Guo, C., & Hu, S. (2022). Serviceability assessment of prestressed concrete cylinder pipes with broken wires: Analytical solution and numerical simulation. *Tunnelling and Underground Space Technology, 126*, 104551.

Zhang, C., Yu, J., & Huang, M. (2012). Effects of tunnelling on existing pipelines in layered soils. *Computers and Geotechnics, 43*, 12–25.

Zhang, L., Zhao, X., Yan, X., & Yang, X. (2017). Elastoplastic analysis of mechanical response of buried pipelines under strike-slip faults. *International Journal of Geomechanics, 17*(4), 04016109.